Chapter 2

Preparation, Characterization and Steady-State Properties of DNS-cytochromes *c*

INTRODUCTION

Fluorescence spectroscopy is effective for studying the conformational changes in proteins because it is very sensitive to the chromophore environment. We have modified *S. cerevisiae* iso-1 cytochrome *c* (cyt *c*), a 108-residue, partially helical, heme protein[1] (**Figure 2.1**) with a dansyl fluorphore (DNS) at the C-terminal helix (C102), at the N-terminal helix (C8), and at the loops (C85) and (C39) (**Figure 2.2**). In the folded states of all four proteins, DNS luminescence intensity and the excited state decay time are strongly quenched by energy transfer to the heme; in unfolded states, fluorescence is partially restored, but to a degree that depends on the position of the label.

The distribution of distances between donor (***D***) and acceptor (***A***) labeled residues in a polypeptide can be extracted from an analysis of fluorescence energy transfer (FET) kinetics.[2] An ensemble of unfolded polypeptides should have a broad ***D-A*** distribution ($P(r)$) (**Figure 2.3**), with a mean value ($\bar{r}$) that increases with the number of residues between ***D*** and ***A***. The many different distances in this ensemble produce a distribution of fluorescence decay rates ($P(k)$) and a highly nonexponential decay profile ($I(t)$) (**Figure 2.3**). By contrast, a folded protein will have a narrow $P(r)$ range, a smaller value of $\bar{r}$, and faster, albeit still nonexponential decays.

We have examined ***D-A*** distance distributions during equilibrium unfolding of cyt *c*. FET kinetics show that, contrary to the two-state model commonly used to analyze the sigmoidal equilibrium unfolding transitions of proteins, the steady-state folded-to-unfolded transitions do not proceed via a two-state equilibrium. The unfolding is heterogeneous for all the different regions of the protein; at equilibrium multiple partially folded species are present.

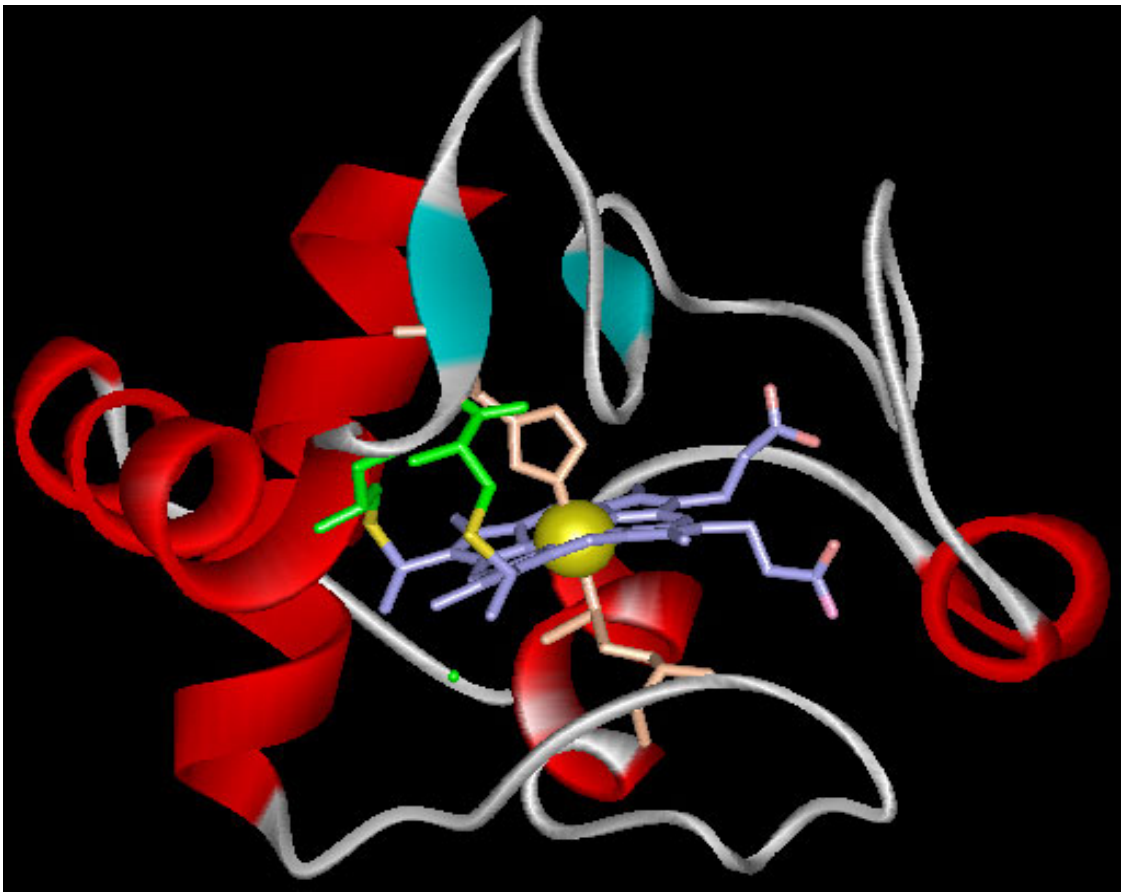

Figure 2.1. *Saccharomyces cerevisiae* cytochrome *c* (iso-1 form, oxidized; C102T mutant; PDB file: 2YCC.pdb) CYS14 and CYS17 covalently bound to the heme are shown in green (except sulfurs which are shown in yellow). The axial ligands (MET80 and HIS18) are pink/orange.

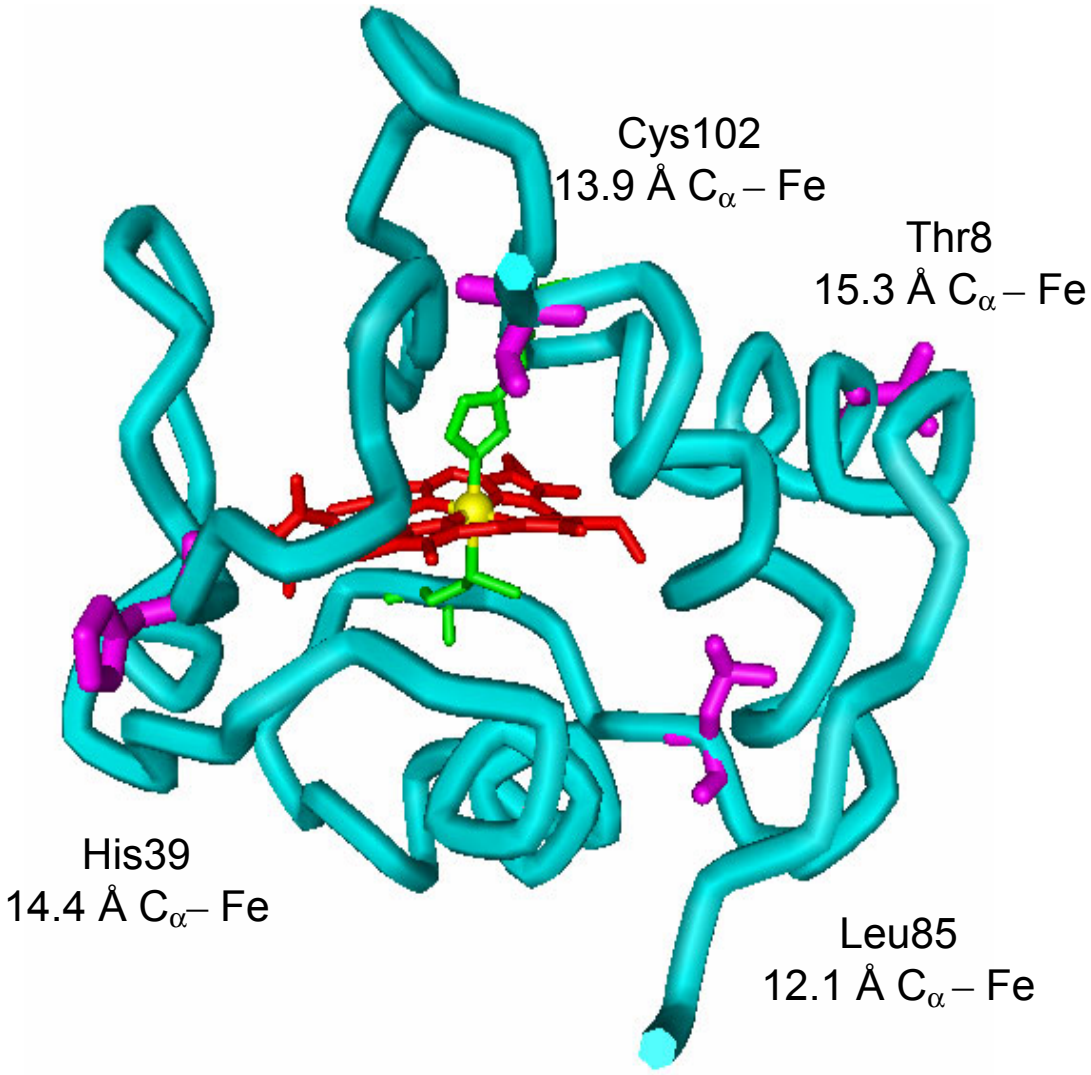

Figure 2.2. The backbone structure of *Saccharomyces cerevisiae* cyt *c.* The cysteine in the wild type (C102) and the residues mutated to cysteine for DNS attachment are shown in purple.

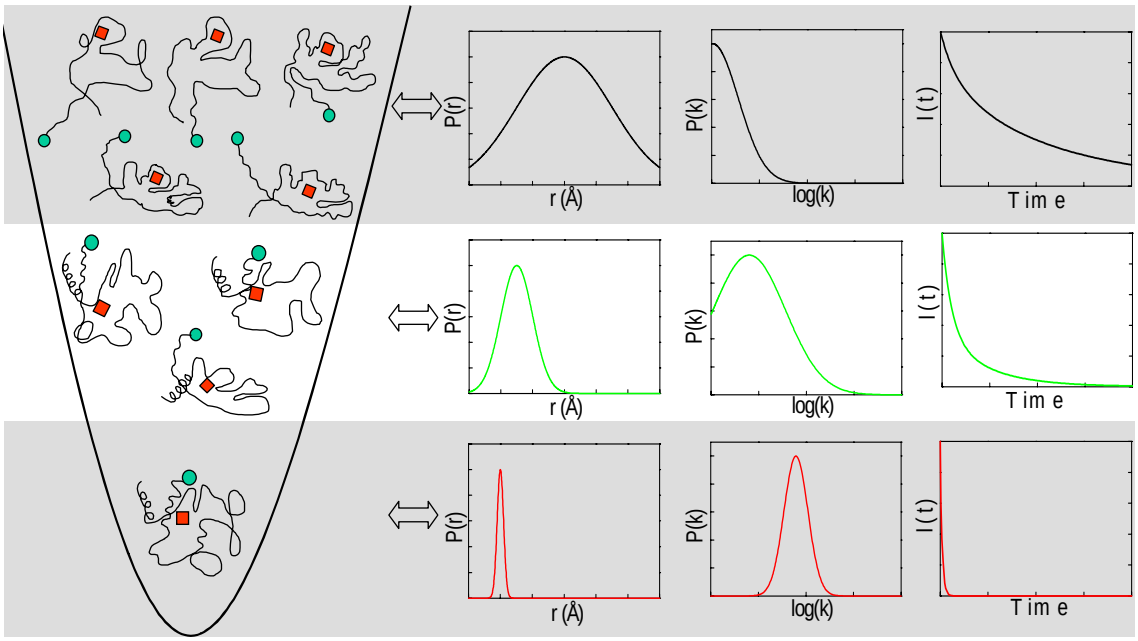

Figure 2.3. Schematic representation of the relationship between polypeptide conformations and fluorescence decay kinetics. An ensemble of unfolded proteins found near the top will have a broad distribution of distances ($P(r)$) between fluorescence energy transfer donors and acceptors. The distance distribution function can be transformed using Eq. 2.15 to a distribution over fluorescence decay rates (k), producing (Eq. 2.14) a slowly decaying fluorescence intensity profile ($I(t)$). An ensemble of folded proteins (bottom) will have narrow distance distribution, and faster excited-state decay.

BACKGROUND

Saccharomyces cerevisiae iso-1 cytochrome *c* (cyt *c*)

Saccharomyces cerevisiae iso-1 cytochrome *c* (**Figure 2.1**) is one of the isozymes of cytochrome *c* that occur in yeast. It is a part of the respiratory electron transport chain and helps to shuttle electrons across a mitochondrial membrane. It is a small 108-residue protein (Mr = 12,708 D) with a cysteine at position 102 (C-terminal α helix).

Although cytochrome *c* is a mitochondrial protein, it is encoded by nuclear genes. The protoheme becomes covalently attached through thioether bonds to Cys14 and Cys17 during post-translational modification. In the folded protein, at physiological pH, His18 and Met80 are the axial ligands to the heme iron.[3,4]

The type of heme, the iron oxidation and the spin state can be characterized by electronic absorption spectroscopy.[4] The Soret band ($\pi \rightarrow \pi^*$ transition located mainly on porphyrin) is centered at 410 nm ($\varepsilon_{410} = 106\times10^3$ $M^{-1}cm^{-1}$) in the folded oxidized protein. It shifts to 408 nm upon unfolding of protein with GuHCl. In the reduced folded protein, the Soret band is centered at 415 nm. The Q band is another transition centered mainly on porphyrin. In the folded oxidized protein it is a broad bump with a maximum ~ 530 nm ($\varepsilon_{530} = 11.2\times10^3$ M^{-1} cm^{-1}). In the folded reduced protein, the Q band has two sharp peaks centered at 520 nm and 550 nm (splitting of electronic transition as a result of vibrational process).[4] The d-d transitions are very weak and not observable.[4]

Fluorescence Energy Transfer (FET)

FET occurs when the emission energy of the donor (***D***) and the excitation energy of the acceptor (***A***) are coupled in resonance interaction. It is a singlet-singlet, nonradiative energy

transfer process theory for which was developed by Theodore Förster.[5] The rate of energy transfer (k_{et}) depends on the decay rate of an unquenched fluorophore ($k_0 = 1/\tau_D$, τ_D is the lifetime of the donor in the absence of acceptor), the distance between the donor and acceptor (r) and the critical length (r_0, Eq. 2.1)

$$k_{et} = k_0\left(\frac{r_0}{r}\right)^6 \tag{2.1}$$

The critical length (r_0) depends on the spectroscopic properties of the donor and acceptor and the refractive index (n) of the surrounding medium.

$$r_0^6 = 8.79\times10^{-5}\frac{\kappa^2\Phi_D J}{n^4}\ (\text{in Å}^6) \tag{2.2}$$

$$J = \int \varepsilon_A(\lambda) F_D(\lambda) \lambda^4 d\lambda \tag{2.3}$$

κ^2 is the geometric factor describing the relative orientation of the donor and acceptor dipoles. κ^2 approaches a limiting value of $^2/_3$ if both donor and acceptor tumble rapidly on the time scale of fluorescence emission. Φ_D is the quantum yield of a donor in absence of acceptor. J is a measure of spectral overlap between the donor fruorescence and acceptor absorption (F_D is the normalized fluorescence intensity of the donor; ε_A is the extinction coefficient of the acceptor). The rate of energy transfer is equal to the decay rate of the unquenched fluorophore (k_0) when the ***D-A*** distance is equal to the critical length (r_0). The efficiency of energy transfer is

$$E = \frac{k_{et}}{k_{et} + k_0} = \frac{r_0^6}{r_0^6 + r^6} \tag{2.4}$$

Hence in the vicinity of r_0, ***D-A*** distances can be determined accurately. Under typical conditions, FET rates can be measured for ***D-A*** distances in the range $0.3\ r_0 \leq r \leq 1.5\ r_0$ (**Figure 2.4**).

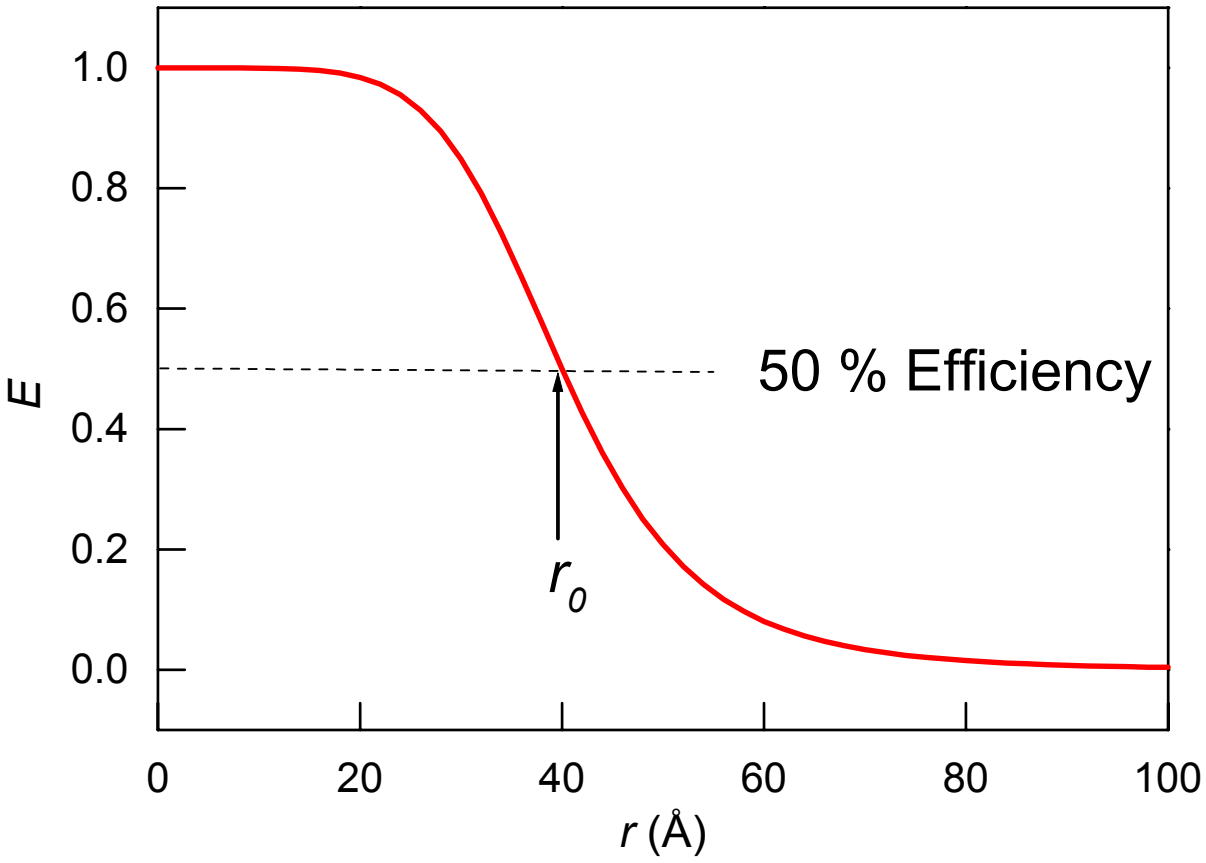

Figure 2.4. Dependence of energy transfer efficiency on critical length r_0 (Eq. 2.4).

MATERIALS AND METHODS

General

Doubly distilled, deionized water was used in media preparations. SD media: 0.67% yeast nitrogen base without amino acids (Difco), 2% dextrose, 0.002% histidine, 0.002% tryptophan. YPD media: 1% bacto-yeast extract (Difco), 2% bacto-peptone (Difco), 2% dextrose. YPG media: 1% bacto-yeast extract (Difco), 2% bacto-peptone (Difco), 3% (v/v) glycerol (reagent grade). TB media: 1.2% bacto-tryptone (Difco), 2.4% bacto-yeast extract (Difco), 4% (v/v) glycerol, 100 mL potassium phosphate buffer (KP_i, pH 7). LB media: 1% bacto-tryptone (Difco), 0.5% bacto-yeast extract (Difco), 1% NaCl, 1 mL NaOH. Culture plates were prepared by adding 2% bacto-agar (Difco) to the desired media. The water used in buffer preparation was purified by passing distilled water through a Barnstead NANOpure purification system equipped with two ion-exchange filters. Specific resistance of water was about 18 MΩ-cm. Protein solutions were concentrated using ultrafiltration units (strirred cells, centripreps, centricons, microcons, Millipore) containing YM3 or YM10 membranes. Absorbance spectra were measured using a Hewlett-Packard 8452A Diode-Array or Cary 14 spectrophotometer. Circular dichroism (CD) spectra were acquired on an Aviv 62ADS spectropolarimeter. Luminescence spectra were measured using a Hitachi F-4500 spectrofluorimeter (λ_{ex} = 355 nm, λ_{obsd} = 400-700 nm) or ISS K2 Multifrequency spectrofluorimeter (λ_{ex} = 355 nm, λ_{obsd} = 400-700 nm). All luminescence spectra were corrected for a background emission and for instrument response. Mass spectral analyses were performed at the Protein/Peptide Microanalytical laboratory in the Beckman Institute at Caltech. DNA plasmids were sequenced at the DNA Sequencing Core Facility in the

Beckman Institute at Caltech. Unless otherwise stated, ion-exchange chromatography was performed using Pharmacia FPLC, Mono S column, NaPi, pH 7, μ 0.1 M, salt gradient 0 to 0.5 M NaCl. Concentrations of cytochromes were determined spectrophotometrically using $\varepsilon_{410} = 106 \times 10^3\ M^{-1}cm^{-1}$.

Protein Derivatization DNS(C102)-cyt *c*

The C102 sulfhydryl group of *S. cerevisiae* iso-1 cytochrome *c* was derivatized with the thiol-reactive fluorophore 5-((((2-iodoacetyl)amino)ethyl)amino)-naphthalene-1-sulfonic acid (1,5-I-AEDANS, Molecular Probes). Fe(III) cyt *c* (50 mg, Sigma) was dissolved in degassed sodium phosphate buffer (NaPi, 2 ml, pH 7.3, μ 0.1 M) and urea (1g) was added to denature the protein. Dropwise addition of a 3-fold molar excess of 1,5-I-AEDANS in water (5 mg/300 mL) proceeded over a 1.5 h time period. After 2.5 h, the reaction was quenched by addition of dithiothreitol (DTT, ICN Biomedical, Inc.). The derivatization reaction was performed in the dark to minimize deleterious photochemical side reactions. Protein was separated from 1,5-I-AEDANS and DTT by gel filtration chromatography (Sephadex G-25, Sigma, bead size 20-80 μm, 5mL/g dry gel, swollen in H_2O, eluted with NaPi, pH 7, μ 0.1 M), oxidized with $K_3Co(C_2O_4)_3$ (a gift of Jason R. Telford) and further purified by ion-exchange chromatography.

Model Compound (1,5 NAC-AEDANS) Synthesis

The N-acetylcysteine derivative of AEDANS was prepared according to a published procedure,[6] with minor modifications. 1,5-I-AEDANS (100 mg, Molecular Probes) was mixed with about 10-fold molar excess of N-acetylcysteine (420 mg, Sigma) in 4 mL of NaP_i

buffer (pH 7, μ 0.1 M) for about 1 h. The solution pH was adjusted to about 7.0 with NaOH (1M) and maintained at this level for an additional 1–2 h. The solution pH was then adjusted to 2.0 with concentrated HCl and the mixture was cooled to 4°C. After about 24 h, a small amount of precipitate had formed, and the solution was rotovapped to dryness. The residue was washed with ether and recrystallized from hot water. The recrystallized material was washed with at least 300 mL of acetone to remove excess N-acetylcysteine and again recrystallized from hot water. The resulting pale yellow-green prismatic crystals were air dried at room temperature.

Cysteine Mutants of Cyt *c*

Protein Expression, Purification and Modification (Yeast Expression System)

Yeast cells (GM-3C-2 cell line) transformed with pING4 plasmid (10.5 kb)[7] bearing the following mutations T8C/C102T ((C8)—cyt *c*) or H39C/C102T ((C39)—cyt *c*) or L85C/C102T ((C85)—cyt *c*) of *S. cerevisiae* iso-1 cyt *c* were from A. G. Mauk, University of British Columbia. The cells from slants were inoculated into 2 mL of SD media supplemented with 50 μg/mL ampicillin and grown aerobically at 30°C with rapid shaking (250 rpm). After a few days of growth, the colonies were plated on YPG plates (50 μg/mL ampicillin) to select for a single colony with a functional cytochrome *c*. The single colonies were inoculated into 2 mL of SD media (50 μg/mL ampicillin) and were grown aerobically at 30°C with rapid shaking (250 rpm) for 3-5 days. The 2 mL preparations were inoculated into 100 mL SD media (50 μg/mL ampicillin). After 5 days of growth, cells and media were inoculated into 10 L of YPG media (50 μg/mL ampicillin) and grown for 5-7 days with rapid shaking at 30°C. For larger preparations, a 60 L fermenter (D. Rees group, Caltech) or a 200

L fermenter (Lawrence M. Tudor, Caltech) was employed. Cell lysis was performed by stirring cells in 1:1 v/w 1 M NaCl, 50 mM NaPi, 1mM EDTA, 0.5:1 v/w ethyl acetate for 36 h at 4°C. The suspensions were centrifuged (GSA rotor, 5k rpm, 45 min, 4°C) and the pellet was discarded. The supernatant was brought to 50% saturation with $(NH_4)_2SO_4$ (316g per 1 L of supernatant). The resulting precipitate was pelleted by centrifugation (GSA rotor, 5k rpm, 45 min, 4°C). The supernatant was filtered through a coarse porosity fritted-disk funnel and washed 4 times with buffer (NaPi 12.5 mM, 1mM EDTA, pH 7) through a YM10 membrane. The contents were added to 300 mL (500 mL for larger-scale preparations) of fast-flow CM52 Sepharose ion-exchange resin (Whatman) prewashed with an equal volume of buffer (NaPi 50 mM, 1mM EDTA, pH 7). The protein was allowed to bind to the resin by stirring the suspension at 4°C for 4 h. The resin was loaded into a column and washed with 1 column volume of buffer (NaPi 50 mM, pH 7). The cytochrome *c* was eluted with a continuous linear salt gradient (0-1 M NaCl, 50 mM NaPi, pH 7). The average protein yield was about 2 mg/L after this purification step. The cytochrome *c* was reduced with dithiothreitol (DTT, ICN Biomedical, Inc.) and purified by ion-exchange chromatography. The sulfhydryl group of the cytochrome *c* variants was derivatized with thiol-reactive fluorophore 5-((((2-iodoacetyl)amino)ethyl)amino)-naphthalene-1-sulfonic acid (1,5-I-AEDANS, Molecular Probes) following the procedure for modification of C102 group in DNS(C102)-cyt *c*.

The sequences of all three cyt *c* mutants were confirmed. The pING4 plasmid was isolated from a selected single colony of yeast cells with Zymoprep Yeast Plasmid Miniprep Kit (Zymoresearch) and amplified in the One Shot Top10F' *E. coli* cells (Invitrogen). The plasmids isolated from *E. coli* cells with QIAGEN Miniprep Kit to a purity of $R_{260/280} \approx 1.7$

(by UV-VIS) were sent to the DNA Sequencing Core Facility (Beckman Institute, Caltech) for sequencing. The primers used for sequencing were

5'-ACATGATATCGACAAA-3'

5'-CAAGTACTCTGACAT-3'

5'-GGACCAACCTTATGTG-3'

5'-GTGTATTTGTGTTTGCG-3'

Protein Expression and Purification (*E. coli* Expression System)

The plasmid pET20b(+) bearing *S. cerevisiae* iso-1-cyt *c* gene (C102S variant) placed after the vector-derived PelB periplasmic leader sequence was constructed by Michele A. McGuirl.[8] It was co-expressed with pEC86[9] in *E. coli* BL21 Star™ (DE3) cells using TB media (60 μg/mL ampicillin, 30 μg/mL chloramphenicol, 37°C) and induced with IPTG ($[IPTG]_{final}$ = 0.4 mM) at the late log phase. Cells were harvested about 6 h after induction. The bright red cell pellets were frozen overnight. BugBuster detergent solution (Novagen, 5 mL/g cell paste) was used to lyse the cells. Benzonase (Sigma) was added to the lysate to reduce viscosity. Protease inhibitor cocktail (Sigma) was added as well. The suspension was centrifuged and the supernatant was collected. The pellet was resuspended in sodium phosphate buffer (10 mM NaPi, pH 7) and centrifuged to recover more protein. The resuspension followed by centrifugation and collection of the supernatant was repeated several times. The resulting crude protein extract was loaded with a peristaltic pump onto a Fast Flow CM-Sepharose (Pharmacia) Econo-column (Biorad) equilibrated with sodium phosphate buffer (10 mM NaPi, pH 7). The column was washed with 2 column volumes of sodium phosphate buffer (10 mM NaPi, pH 7). The protein was eluted with a stepwise salt

gradient (0 to 0.5 M NaCl, 10 mM NaPi, pH 7). *S. cerevisiae* iso-1 cyt *c* eluted at 0.33 M NaCl. The protein yield was 8-15 mg/L after this purification step. The protein was reoxidized with $K_3Co(C_2O_4)_3$ and purified by ion-exchange chromatography. This variant was named WT* and was found to lack trimethylation at lysine 72[10] (electrospray MS, Mr = 12,651).

Preparation of GuHCl Solutions

Guanidinium hydrochloride (GuHCl, USB or Sigma, highest purity) stock solution (6 M) was prepared in sodium phosphate buffer (NaPi, pH 7, μ 0.1 M) and its pH was adjusted to 7.0-7.2 using concentrated aqueous NaOH. To achieve intermediate GuHCl concentrations, the appropriate aliquots of GuHCl stock solution and sodium phosphate buffer (NaPi, pH 7, μ 0.1 M) were mixed. The pH of each solution was adjusted to 7.0-7.2 using concentrated aqueous NaOH. PreciseGuHCl concentrations were determined from the empirical relationship between [GuHCl] and the solution refractive index.[11]

$$[\text{GuHCl}] = 57.147*\Delta N + 38.68*\Delta N^2 - 91.60*\Delta N^3$$

where ΔN is the difference in the refractive index between each GuHCl solution and water (or buffer). The refractive index of sodium phosphate buffer (NaPi, pH 7, μ 0.1 M) was determined to be 1.335 (NANOpure water 1.333). Refractive index measurements were made using Milton Roy Abbe-3L Refractometer.

Equilibrium Unfolding

For equilibrium unfolding experiments, small amounts of concentrated protein were added to 700 μL - 1 mL aliquots of pH-adjusted GuHCl solutions. The samples were equilibrated at

23°C for at least 10 min before carrying out the measurement. The temperature was kept at 23°C by a Peltier temperature element in absorbance and CD measurements, and by circulating temperature-controlled water in fluorescence intensity measurements. For fluorescence lifetime and intensity experiments, the aliquots of pH-adjusted GuHCl solutions were purged with argon. The cuvette was not rinsed between the samples. The pH and GuHCl concentration of each solution was rechecked after completion of an unfolding experiment.

Denatured State pH Titration of Heme-Histidine Ligation

The titration was carried out in the presence of 1.4 M GuHCl in 50 mM acetate buffer. The initial protein concentration was about 7 μM. The titration was performed on a single sample without removing the cuvette containing the sample from the cuvette holder of a Hewlett-Packard 8452 diode array spectrophotometer. The pH was raised from 2.35 to about 7 by adding small amounts of concentrated aqueous NaOH. The solution was constantly stirred and the pH was monitored *in situ*. The temperature was maintained at 23°C by a Peltier Temperature Control Accessory (Hewlett-Packard). The absorbance spectrum at each pH was measured and later the absorbance was adjusted for dilution. The pH dependence of the absorbance at 396 nm was fit to the Henderson-Hasselbalch equation (Eq. 2.5) [12,13] using Origin software:

$$A_{396} = \frac{A_{396,LS} + A_{396,HS} * 10^{n(pKa-pH)}}{1 + 10^{n(pKa-pH)}} \qquad (2.5)$$

where A_{396} is the absorbance (λ_{obsd} = 396 nm) at a given pH, $A_{396,LS}$ is the absorbance (λ_{obsd} = 396 nm) of the low spin heme, $A_{396,HS}$ is the absorbance (λ_{obsd} = 396 nm) of the high spin heme, pK_a is the midpoint of the transition, and n is the number of protons involved.

Thermal Unfolding

The buffer for the native-to-thermally denatured state transition was sodium phosphate (NaPi, pH 7, μ 0.1 M). The cuvette was capped and sealed with parafilm throughout the experiment. The solution in the cuvette was stirred at all times during an experiment. The ellipticity at 222 nm was measured between 25°C and 80°C every 1°C. The time between successive data points was about 8 min. Reversibility was checked by running the reaction in reverse, back to the initial temperature, or by cooling the sample to the initial temperature and revisiting a few data points and comparing those to the initial values.

Förster Distance

The value of overlap integral (J, Eq. 2.3) for the DNS-heme donor-acceptor pair was determined based on 1,5 NAC-AEDANS fluorescence and DNS(C102)-cyt *c* absorption. The solution refractive index (n) was taken to be 1.34.

FET Kinetics

Fluorescence decay measurements were performed using the third harmonic of a regeneratively amplified, mode-locked Nd-YAG laser (Coherent Antares, 355 nm, 50 ps, 0.5 mJ)[14] for excitation and a picosecond streak camera (Hamamatsu C5680) for detection. Magic-angle excitation and collection conditions were employed throughout.[15] DNS

fluorescence was selected with a long-pass cutoff filter (>430 nm) and collected at a 90º angle to the excitation beam. The C5680 was used in photon counting mode. The fluorescence decay signals were acquired with 1-50 μM protein solutions. For time-resolved fluorescence anisotropy measurements, the polarizer was parallel to the excitation polarization direction. The fluorescence anisotropy decay curves were collected with parallel (($I_{||}(t)$) and perpendicular ($I_{\perp}(t)$) orientations of an analyzing polarizer. Protein samples were purified by ion-exchange chromatography immediately before the measurements. The time-dependent anisotropy was evaluated using Eq. 2.6.

$$r(t) = \frac{I_{||}(t) - I_{\perp}(t)}{I_{||}(t) - 2I_{\perp}(t)} \tag{2.6}$$

The sensitivity of the detection system (G-factor) for vertically and horizontally polarized light was determined with 1,5 NAC-AEDANS model compound in buffer solution (NaPi, pH 7, μ 0.1 M). The G-factor was found to be 1.0.[15]

Data Analysis

Equilibrium Unfolding

A two-state model was used to fit equilibrium unfolding data. The model assumes that in the highly cooperative process of folding/unfolding, only fully folded and fully unfolded states are populated at equilibrium.

Folded ↔ Unfolded

Therefore,

$$f_U + f_F = 1 \tag{2.7}$$

at any point of the folding/unfolding curve, where f_U and f_F are the fractions of protein present in unfolded and folded form respectively. The observed value of some physical property y is then described by

$$y = f_U\, y_U + f_F\, y_F \tag{2.8}$$

Combining Equations (2.7) and (2.8) gives

$$f_U = (y_F - y)/(y_F - y_U) \tag{2.9}$$

The equilibrium constant is

$$K_F = f_F / f_U = (1 - f_U)/f_U = (y - y_U)/(y_F - y) \tag{2.10}$$

$$\Delta G_F = -RT\ln K_F = -RT\ln((y - y_U)/(y_F - y)) \tag{2.11}$$

ΔG_F is the folding free energy in presence of denaturant, R is the gas constant (1.987 cal/molK). Values of y_F and y_U in the transition region are obtained by extrapolating from post- and pre- transitional regions.[16] ΔG_F (H_2O) (free energy of folding in the absence of denaturant) is found from equation (2.12) which assumes that the linear dependence of ΔG_F on denaturant continues to zero denaturant concentration.

$$\Delta G_F = \Delta G_F\,(H_2O) - m[D] \tag{2.12}$$

where [D] is the denaturant concentration and *m* characterizes the steepness of the transition. At the midpoint, the denaturant concentration $[D]_{1/2} = \Delta G_F\,(H_2O)/m$. The Equation (2.13) describes the entire folding/unfolding curve, the best fit to which can be found by varying the following 6 parameters: y_F, m_F, y_U, m_U, $[D]_{1/2}$, m.[16]

$$y = \{(y_F + m_F[D]) + (y_U + m_U[D] \times \exp[m \times ([D]-[D]_{1/2})/RT]\}/ (1 + \exp[m \times ([D]-[D]_{1/2})/RT]). \tag{2.13}$$

FET Kinetics

In order to extract distributions of ***D-A*** distances from the luminescence decay kinetics, we must first obtain *P(k)* by inverting the discrete Laplace transform that describes *I(t)* (Eq. 2.14).

$$I(t) = \sum_{k=k_0}^{\infty} P(k)\exp(-kt) \tag{2.14}$$

Transformation to a probability distribution over *r* (*P(r)*) is readily accomplished using Eq. 2.15.[5]

$$k = k_0 + k_0\left(\frac{r_0}{r}\right)^6 \tag{2.15}$$

The difficulty in obtaining *P(r)* arises in the first step because numerical inversion of *I(t)* is extremely sensitive to noise.[17] Regularization methods that impose additional constraints on the properties of *P(k)* have been developed to stabilize inversion problems of this type. The simplest constraint that applies to FET kinetics data is that $P(k) \geq 0(\forall\ k)$. Data were fit using MATLAB (The Math Works, Inc.) algorithm (LSQNONNEG) that minimized the sum of the squared deviations (χ^2) between observed and calculated values of *I(t)*, subject to a non-negativity constrained. LSQNONNEG fitting produced narrow *P(k)* distributions with relatively few nonzero components. Information theory suggests that the least biased solution to this inversion problem minimizes χ^2 and maximizes the breadth of *P(k)*.[17] This regularization condition can be met by maximizing the Shannon-Jaynes entropy of the rate-constant distribution $S = -\sum_k P(k)\ln\{P(k)\}$, implicitly requiring that $P(k) \geq 0\ (\forall\ k)$.[18] Maximum entropy (ME) fitting produced stable and reproducible inversions for Eq. 2.14. The balance between χ^2 minimization and entropy maximization was determined by

graphical L-curve analysis.[19] The *P(k)* distributions from ME fitting were broader than those obtained with LSQNONNEG fitting but exhibited comparable maxima. The results from LSQNONNEG fitting for DNS(C102)-cyt *c* are shown in **Figure S.2.1** (Supporting Information). The FET kinetics for DNS(C102)-cyt *c* are also well represented by a biexponential function (**Figure S.2.2**, Supporting Information). A simple coordinate transformation was used to recast the *P(k)* results obtained from ME and LSQNONNEG fitting as probability distributions over *r*.

RESULTS AND DISCUSSION

Model Compound (1,5 NAC-AEDANS) Characterization

The model compound, N-acetylcysteine derivative of 1,5-AEDANS (**Figure 2.5**), was synthesized and characterized. It was used to estimate the value of k_0 (Eq. 2.15). The purity of the model compound was determined by HPLC and electrospray MS (Mr = 468 for a negative ion; Mr = 490 for a negative ion and one H substituted by Na ion) (**Figure 2.6**) plus independently by LC/MS (data not shown). As determined by LC/MS, the purity of the model compound was 92%. The UV-VIS absorbance and fluorescence spectra of the model compound (**Figure 2.7**) agreed well with those published in literature.[6] The lifetime of the model compound was 10.2 ns ($k_0 = 9.81 \times 10^7 s^{-1}$) in phosphate buffer (NaPi, pH 7, μ 0.1 M) and did not show any dependence on [GuHCl] up to 6 M.

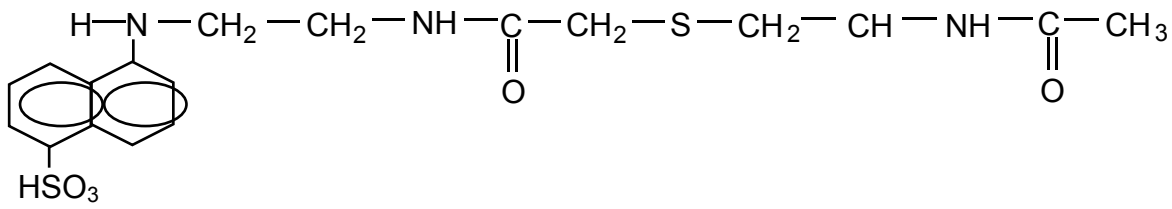

Figure 2.5. Model compound: 1,5 NAC-AEDANS.

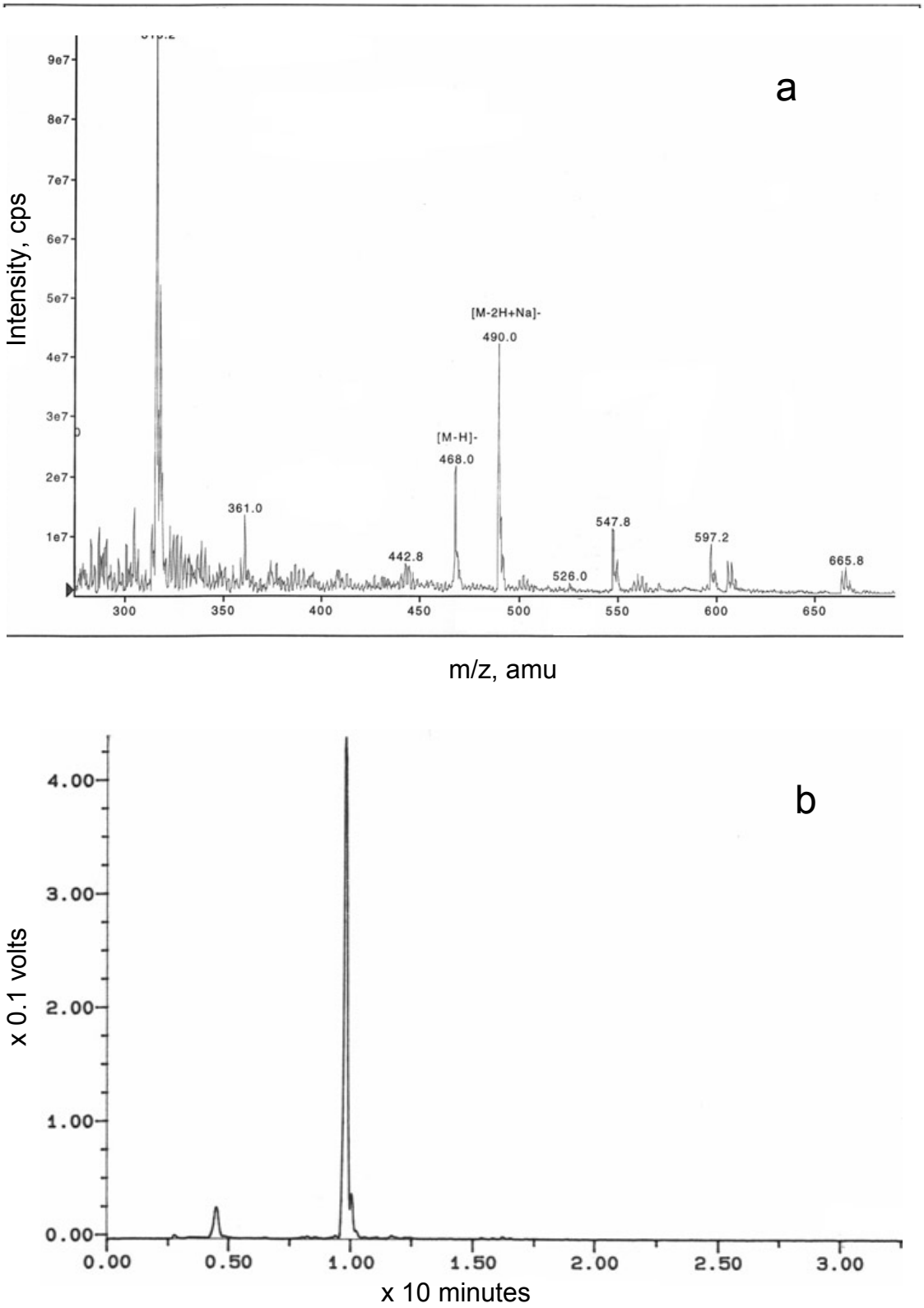

Figure 2.6. 1,5 NAC-AEDANS; (a) electrospray MS; negative ion; mass range: 100.0-800.0 by 0.2 amu; dwell: 0.5 ms; pause: 5.0 ms; 15 scans
(b) c18 reversed phase HPLC; λ_{obsd}=336 nm; gradient: 60% acetonitrile in 30 min.

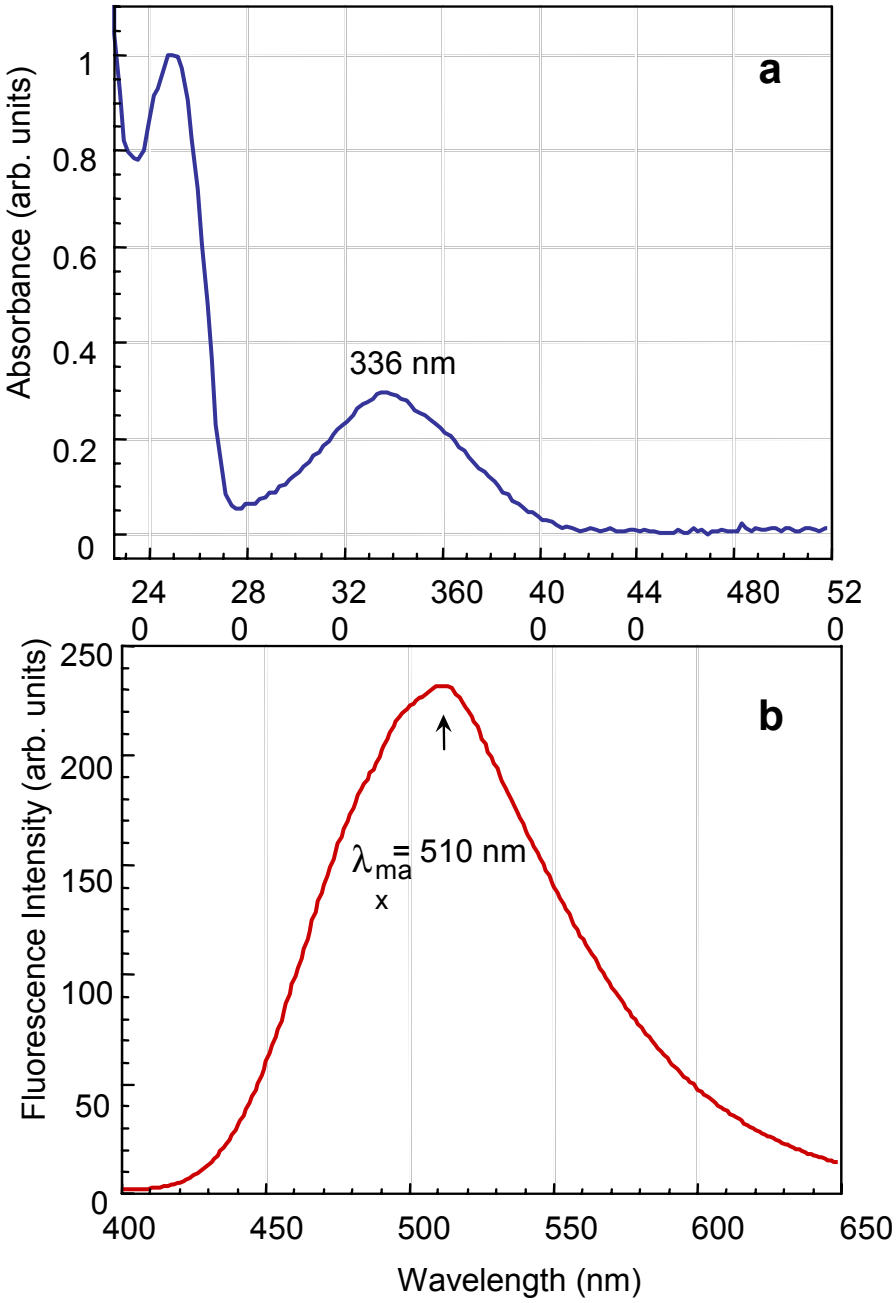

Figure 2.7. 1, 5 NAC - AEDANS (55 μM, 16 mM NaPi, pH 7, 20 °C) (ε_{250} = 18×10^3 M^{-1} cm^{-1} (Kotlyar, Borovok, BBA 1321(1997) 221-228); (a) absorption spectrum; (b) fluorescence spectrum. λ_{ex} = 336nm. Power: 550 V, lamp current: 18 A, slits (ex, em) = 1.0. Corrected for background emission and for instrument response.

Preparation and Characterization of DNS-cytochromes *c*

DNS(C102)-cyt *c*

Figure 2.8 shows a typical FPLC trace (λ_{obsd} = 280 nm) for separating DNS(C102)-cyt *c* (absorption spectrum**, Figure 2.9.** The peak at 260 nm is due to DNS label) from unmodified protein. DNS(C102)-cyt *c* elutes at lower [NaCl] due to a negatively charged sulfonate group of the DNS fluorophore. The purity of modified cyt *c* was confirmed by mass spectrometry (**Figure 2.10**, Mr = 13,015.9 for a singly modified protein) and SDS/PAGE electrophoresis. Tryptic digests with subsequent HPLC separation and MS fragment characterization were performed during initial labeling experiments. The results suggested that only sulfur (C102) would acquire label and no double labeling occurred. This was not surprising as the pH at which labeling was performed (pH ~7.2) was low enough to make only sulfur sufficiently nucleophilic. Endoasp-N protease digest with subsequent HPLC separation was also performed. A single peptide fragment DLITYLKKAXE (where X is a modified residue) with m/z = 1603.75 and 336 nm absorbance showed up in the digest of the modified protein, but was absent in the digest of unmodified protein. The peptide sequence was confirmed by tandem mass spectrometry. The X residue showed mass 409 and was presumed to be dansylated cystein.

DNS(C39)-cyt *c*

The FPLC ion-exchange chromatogram of (C39)-cyt *c* is shown in **Figure 2.11.** This final purification step efficiently separates the (C39)-cyt *c* (major peak, Mr = 12,673;

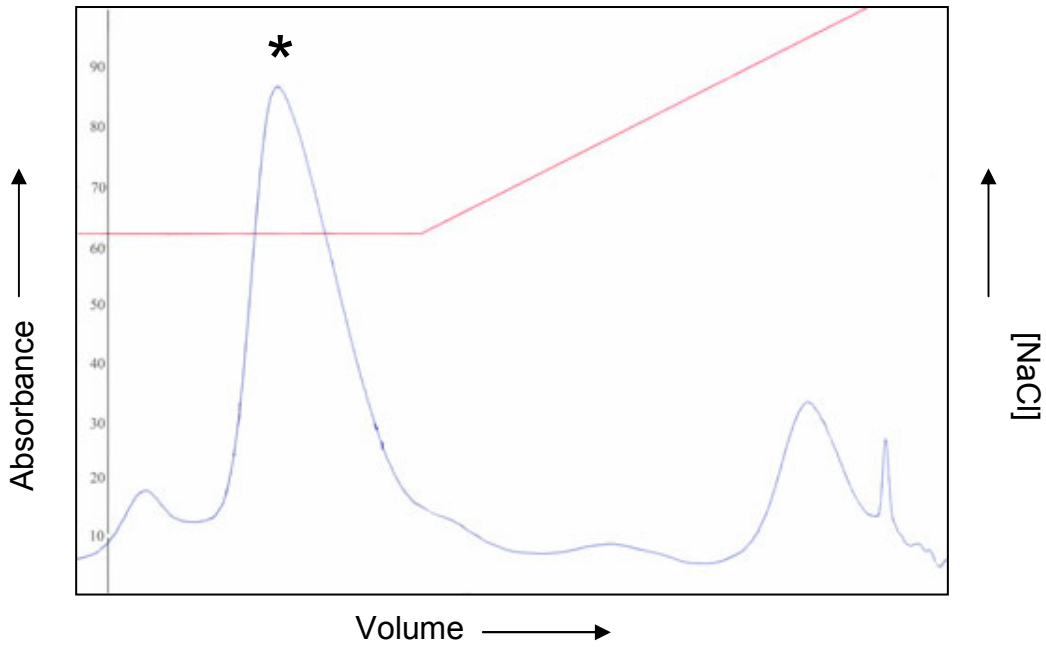

Figure 2.8. Typical ion-exchange chromatogram for the purification of DNS(C102)-cyt *c*. Peak identified by * is the labeled product.

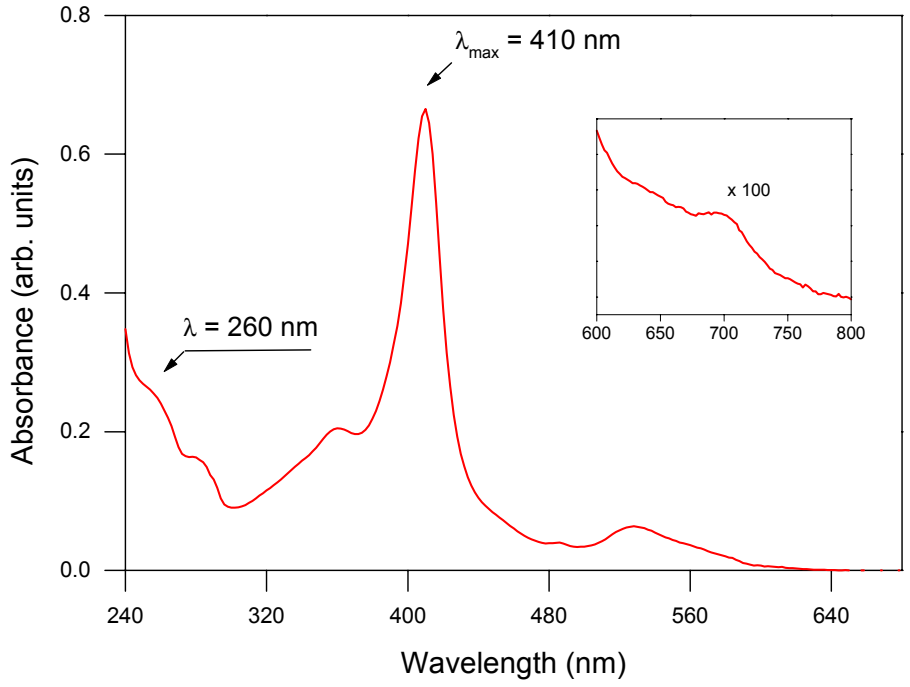

Figure 2.9. Typical absorption spectrum of DNS(C102)-cyt *c* (NaPi, pH 7.2, μ 0.1 M, 21 °C). A peak at λ = 260 nm is from DNS label. Insert is a close-up of Met(80)→Fe(III) transition (λ = 695 nm).

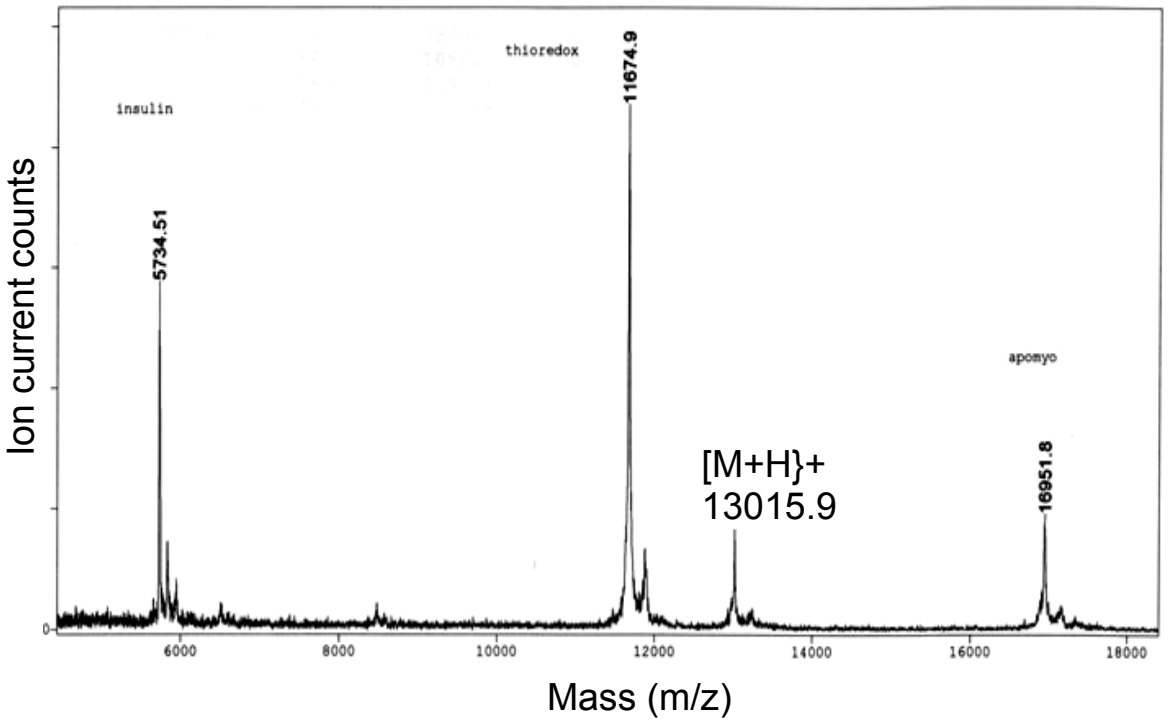

Figure 2.10. PPMAL. DNS(C102)-cyt *c* (Mr = 13015.9) plus calibration standards; method: DEL12K; mode: liner; neg. ions: off; accel. volts: 20000; grid voltage: 90.0005; guide wire voltage: 0.015%; scans averaged: 178; pressure:6.98e-08; low mass gate: 900.0; mirror ratio: 1.1000; timed ion selector 26.4.

Figure 2.12, electrospray MS) from N-acetylated product (Mr = 12,715; **Figure 2.13**, electrospray MS) eluting before the major peak. The FPLC ion-exchange separation for DNS(C39)-cyt *c* from unreacted protein is shown in **Figure 2.14**. Mr for the modified product is 12,979 (**Figure 2.15**). The absorption spectrum of this variant was identical to that for DNS(C102)-cyt *c*.

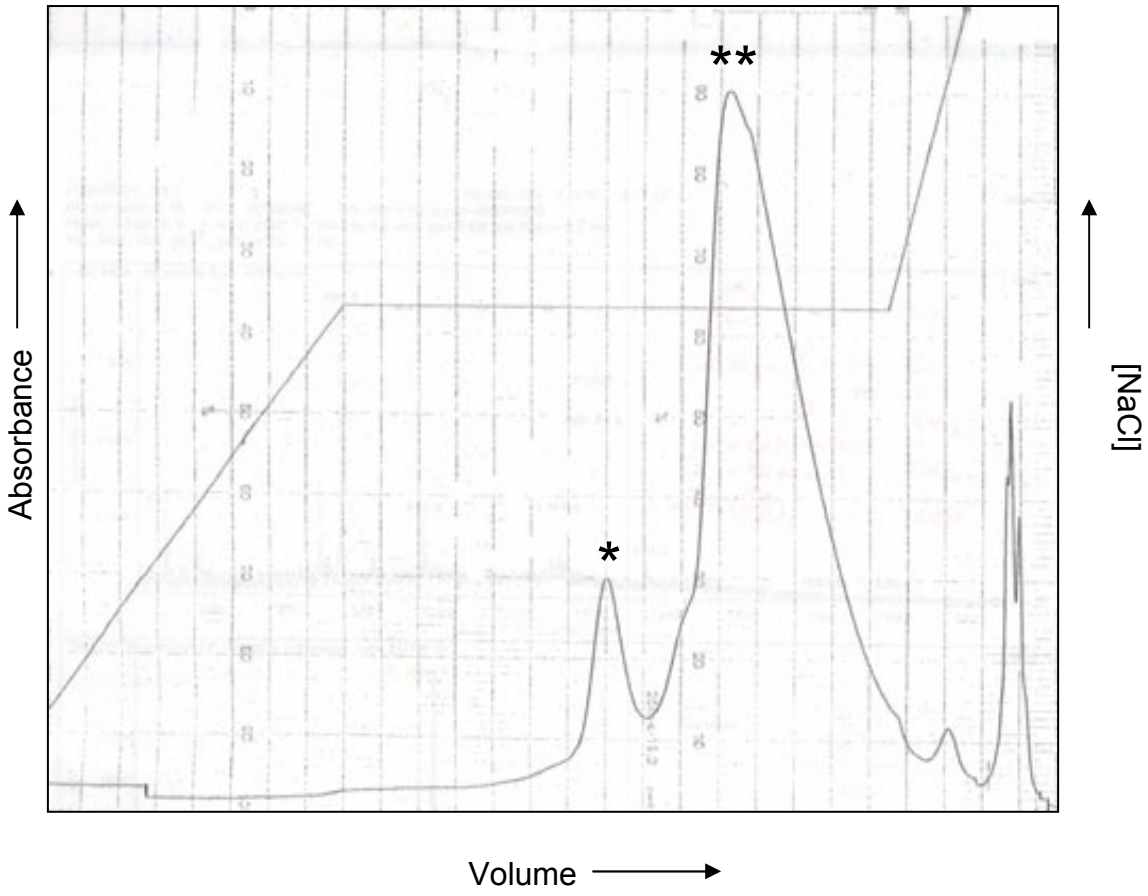

Figure 2.11. Typical ion-exchange (FPLC MonoS) chromatogram for the purification of (C39)-cyt *c*. Peak identified by * is the variant with acetylated N-terminus. Peak identified by ** is pure (C39)-cyt *c*.

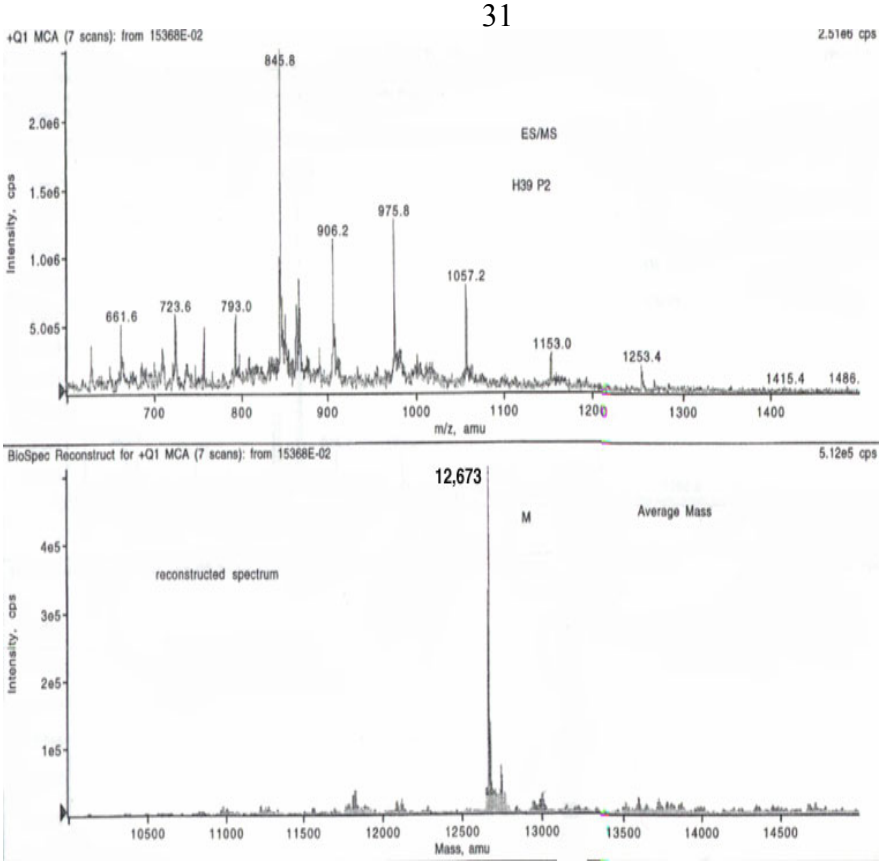

Figure 2.12. Electrospray MS. (C39)-cyt *c.* Mr = 12,673.

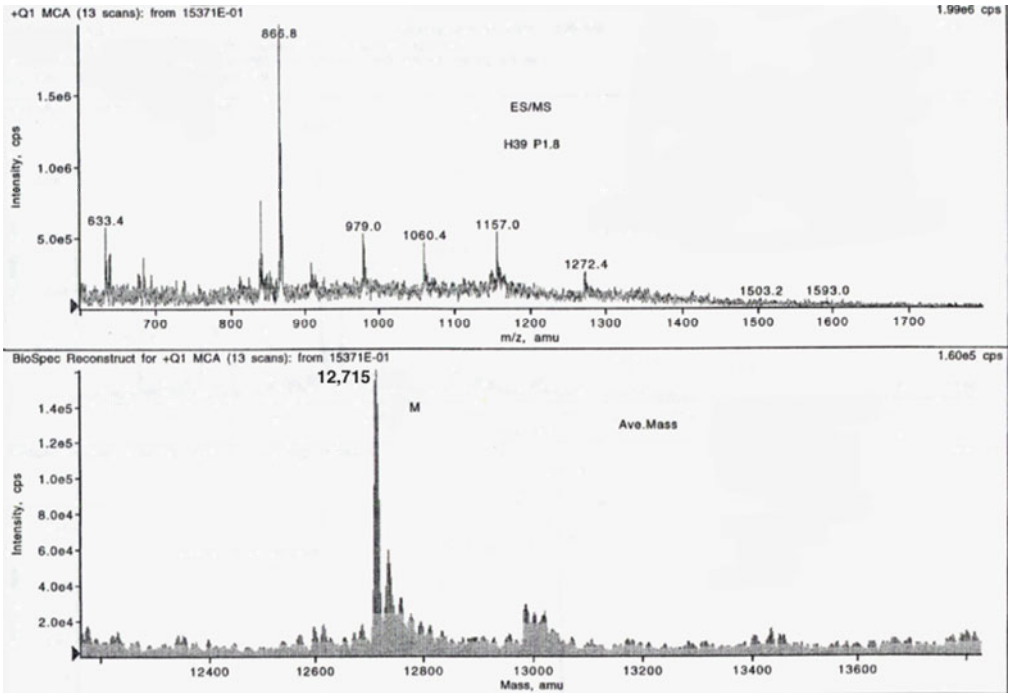

Figure 2.13. Electrospray MS. (C39)-cyt *c.* N-acetylated. Mr = 12,715.

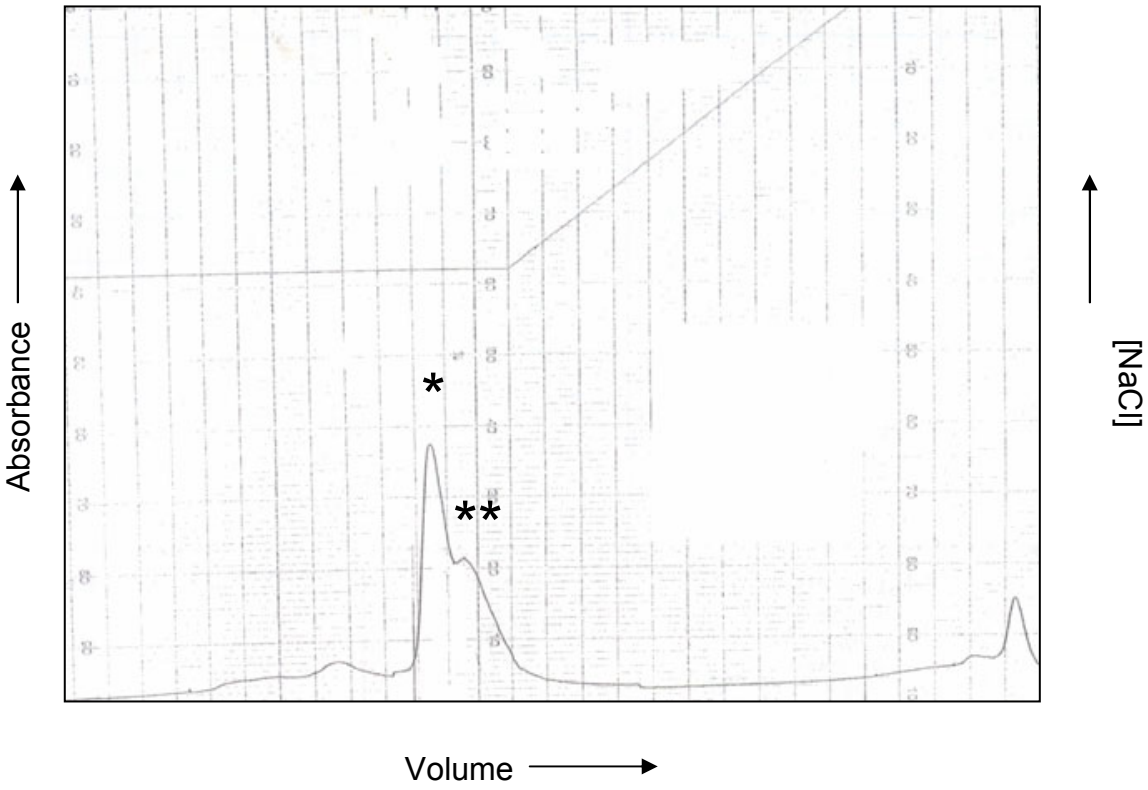

Figure 2.14. Typical ion-exchange (FPLC Mono S) chromatogram for the separation of DNS(C39)-cyt *c*. Peak identified by * is the labeled product and peak identified by ** is unreacted protein.

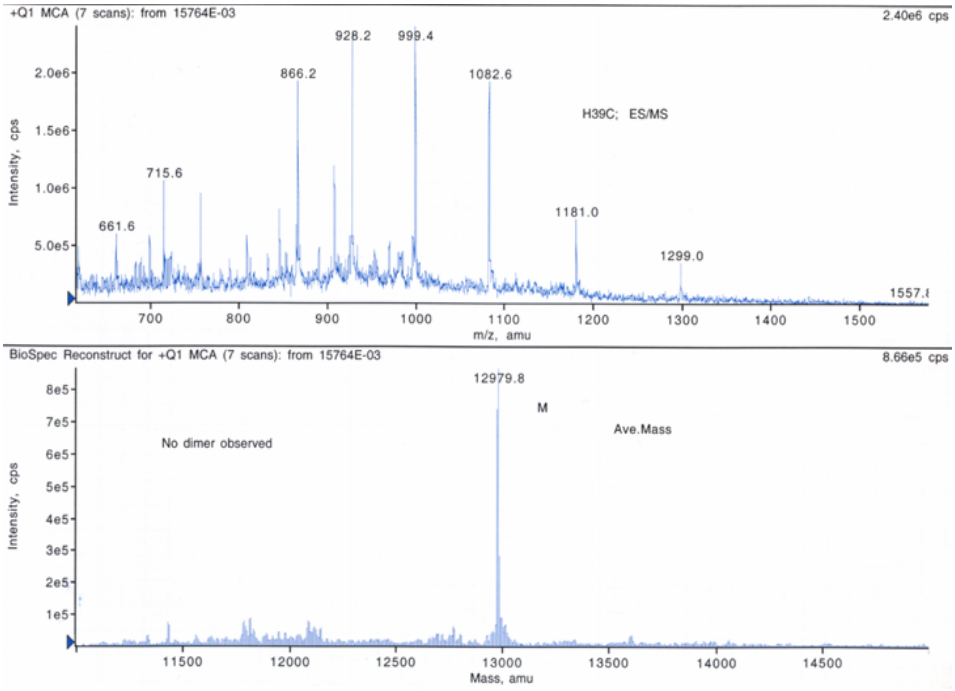

Figure 2.15. Electrospray MS. DNS(C39)-cyt *c*. Mr = 12,979.8.

DNS(C85)-cyt *c*

The FPLC ion-exchange chromatogram for separating DNS(C85)-cyt *c* from unlabeled protein is shown in **Figure 2.16**. The molecular weight of DNS(C85)-cyt *c* was 13,002 (**Figure 2.17**) as determined by mass spectral analysis. The Soret transition for this variant is blue-shifted by about 2 nm compared to DNS(C102)-cyt *c*. This shift is not a consequence of labeling and is observed for an unlabeled protein as well.

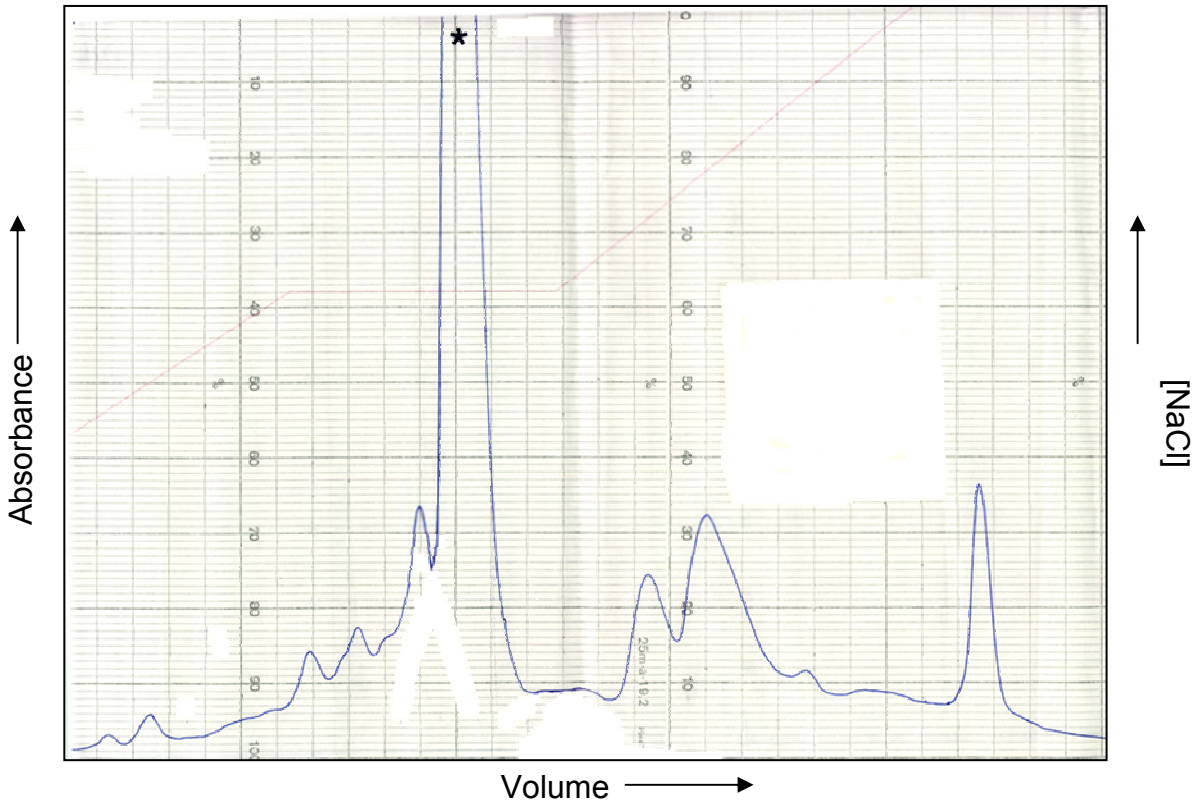

Figure 2.16. Typical ion-exchange (FPLC Mono S) chromatogram for the separation of DNS(C85)-cyt *c*. Peak identified by * is the labeled product.

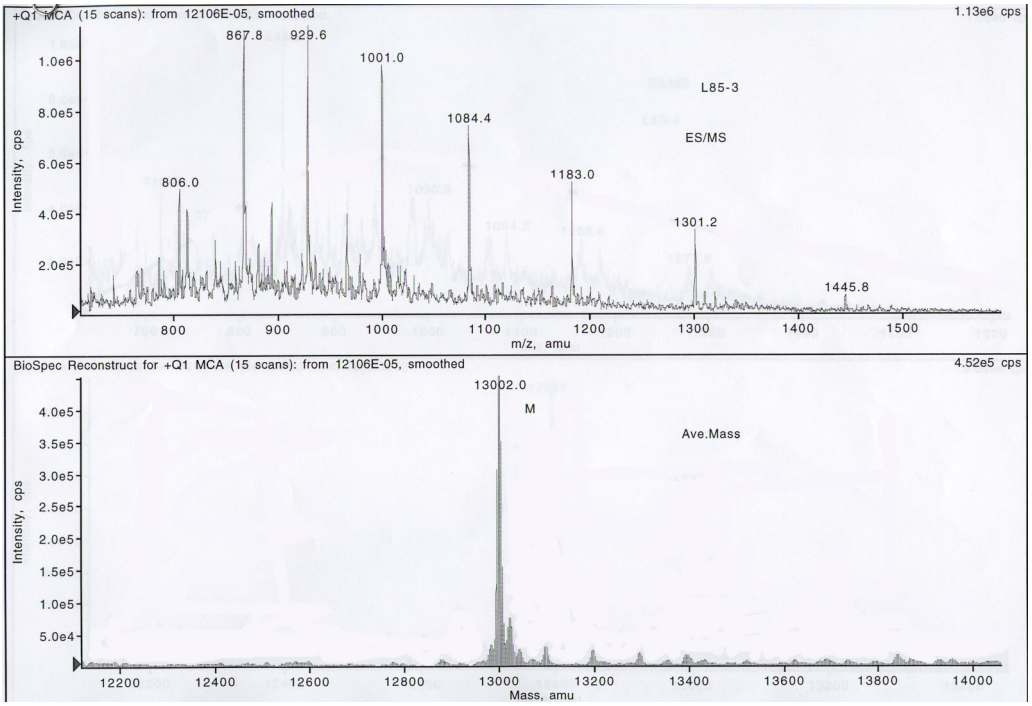

Figure 2.17. Electrospray MS. DNS(C85)-cyt *c*. Mr = 13,002 .

DNS(C8)-cyt *c*

The FPLC ion-exchange chromatogram for separating DNS(C8)-cyt *c* from unlabeled protein is shown in **Figure 2.18**. The molecular weight of DNS(C8)-cyt *c* was 13,012 (**Figure 2.19**) as determined by mass spectral analysis. DNS(C8)-cyt *c* showed no appreciable change in fluorescence intensity upon unfolding with GuHCl and no further work was pursued with this variant.

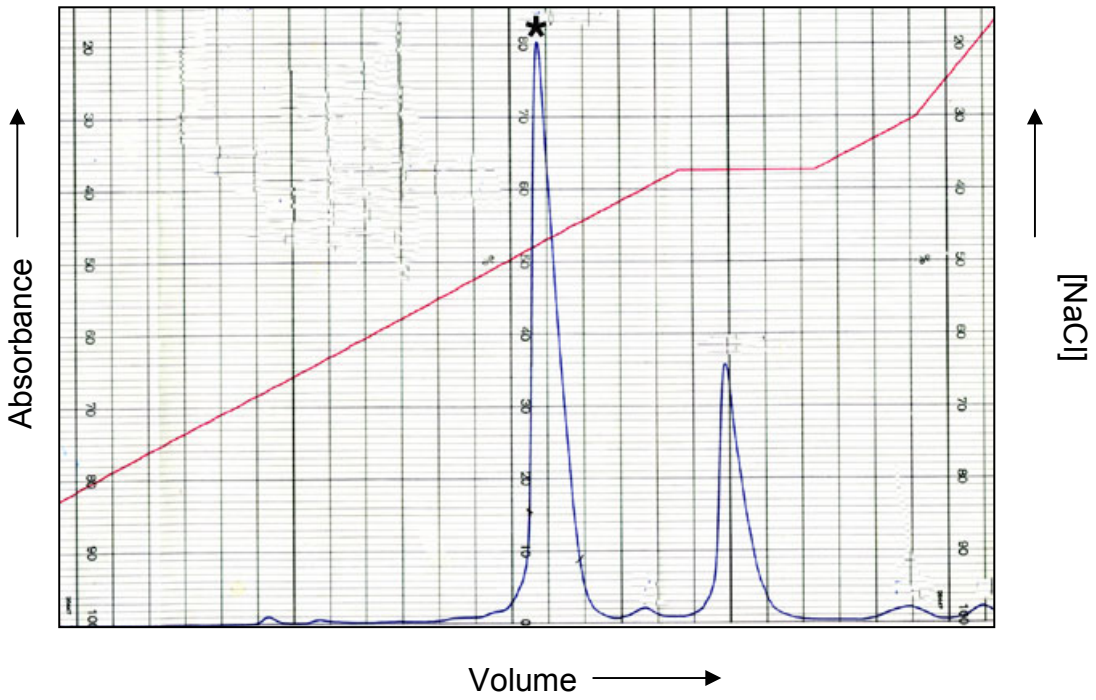

Figure 2.18. Typical ion-exchange (FPLC Mono S) chromatogram for the separation of DNS(C8)-cyt *c.* Peak identified by * is the labeled product.

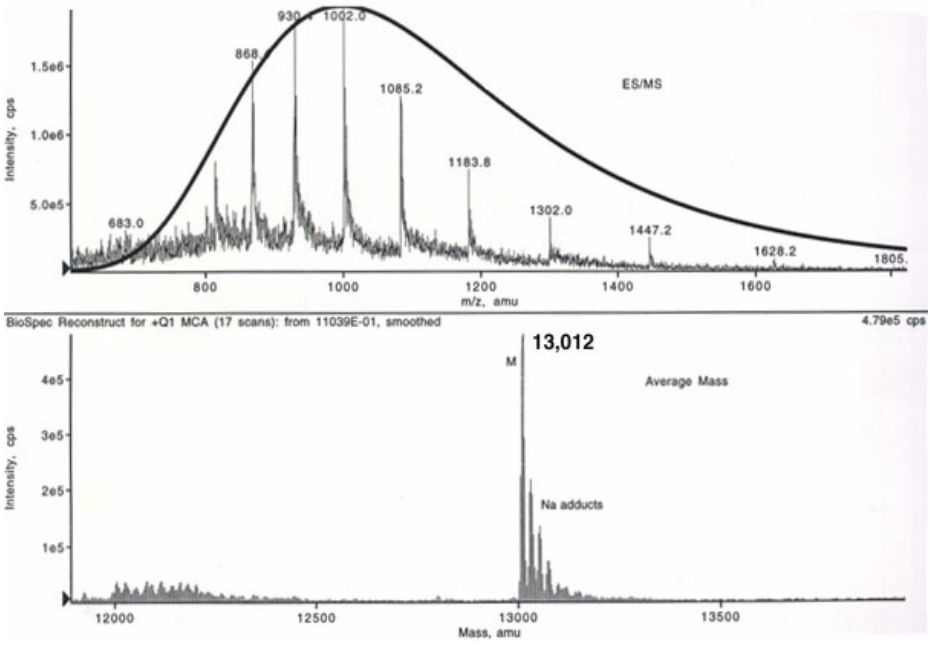

Figure 2.19. Electrospray MS. DNS(C8)-cyt *c.* Mr = 13,012 .

Denatured State pH Titration of Heme-Histidine Ligation of DNS(C102)-cyt *c*

In the folded protein at neutral pH, an imidazole nitrogen (H18[19a]) and a thioether sulfur (M80) axially ligate the heme iron. The nitrogenous base of an amino acid side chain (pH 7: H26, H33, H39) replaces M80 in the guanidinium hydrochloride unfolded protein.[20] Upon lowering the pH, the non-native histidine is protonated and the bond to the heme iron is broken. The spectral changes accompanying this transition for DNS(C102)-cyt *c* are shown in **Figure 2.20**. The Soret band shifts from 408 nm to 396 nm. The absorbance at 396 nm continues to increase as pH is lowered further. The absorbance at 396 nm plotted as function of pH (**Figure 2.21**) displays a transition with a single inflection point at pH 4.3. The transition involves approximately one proton (0.93). For yeast cytochrome *c* all different histidines (H26, H33, H39) have equal affinities for the heme.[13] The observed pK_a for the wild type protein (C102S) is 4.67($\pm$0.03).[12]

Thermal Stability

To determine if presence of DNS affects the thermal transition of cyt *c*, the change in CD at 222 nm was followed as temperature was increased from 25ºC to 80ºC (**Figure 2.22, Figure 2.23, Figure 2.24**). For all modified cyt *c* mutants, the CD melting curve showed a cooperative transition. For the WT*, the midpoint was 59ºC. For DNS(C102)-cyt *c*, a midpoint at 51ºC was observed. For DNS(C85)-cyt *c*, a midpoint was at 49ºC. For DNS(C39)-cyt *c*, a midpoint at 58ºC was observed. The transition for DNS(C39)-cyt *c* was as reversible as the transition for the WT*. The transitions for DNS(C102)-cyt *c* and DNS(C85)-cyt *c* were less reversible compared to the WT*.

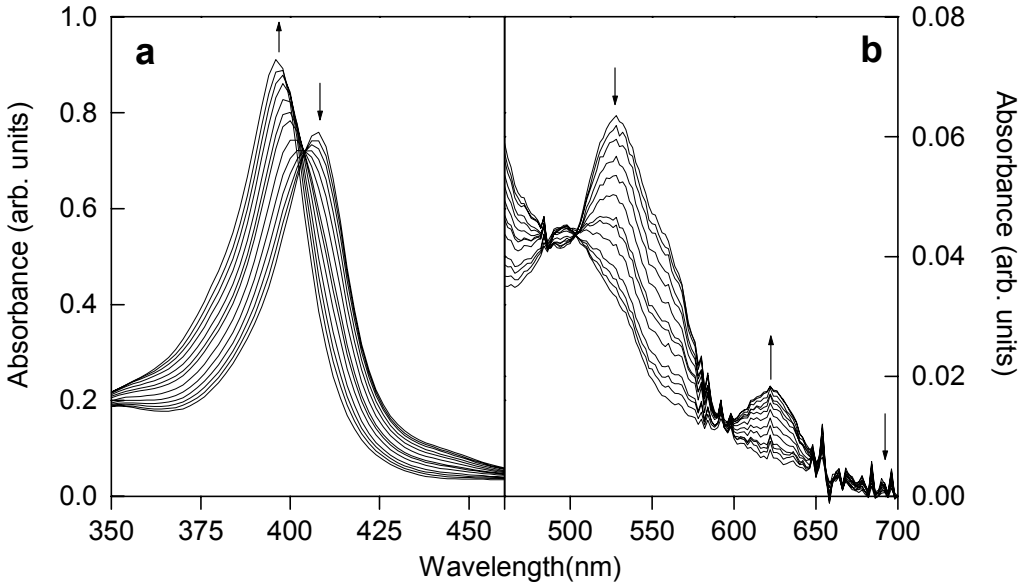

Figure 2.20. pH dependence of the visible absorption spectrum of denatured (1.44 M guanidine-HCl) DNS(C102)-cyt *c*. (a) Soret band region. (b) Q-band region. The concentration of protein was 7 μM. The arrows indicate spectral changes as the pH is lowered. The spectral changes are characteristic of a low to high spin transition.

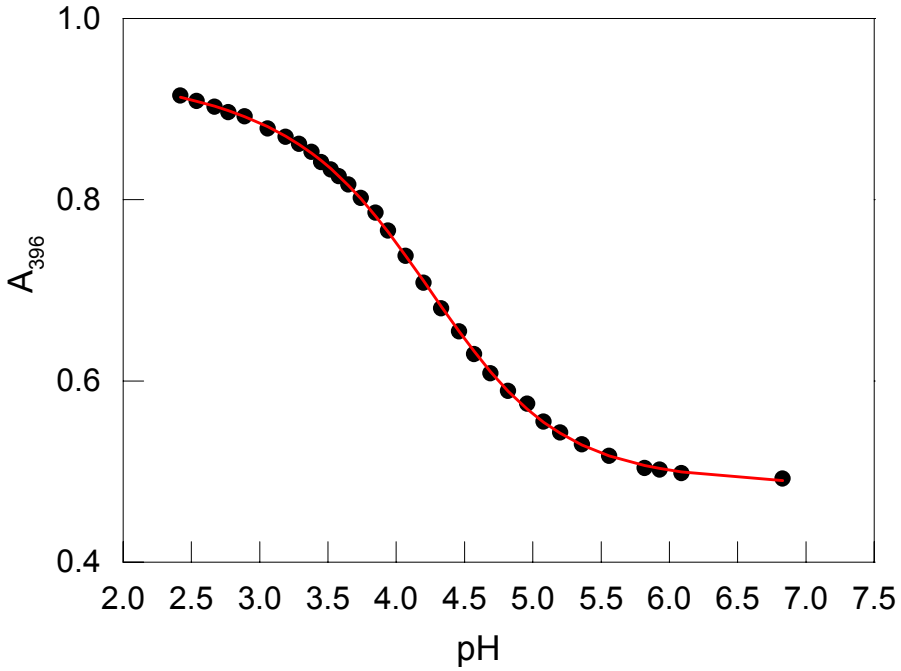

Figure 2.21. Titration of heme-histidine ligation in the denatured state (1.44 M guanidine-HCl) for DNS(C102)-cyt *c*. The continuous line is a fit to a multiproton form of the Henderson-Hasselbalch equation. The data were collected at 22ºC in presence of 50 mM acetate buffer. The concentration of protein was 7 μM. The pH at the midpoint is 4.3.

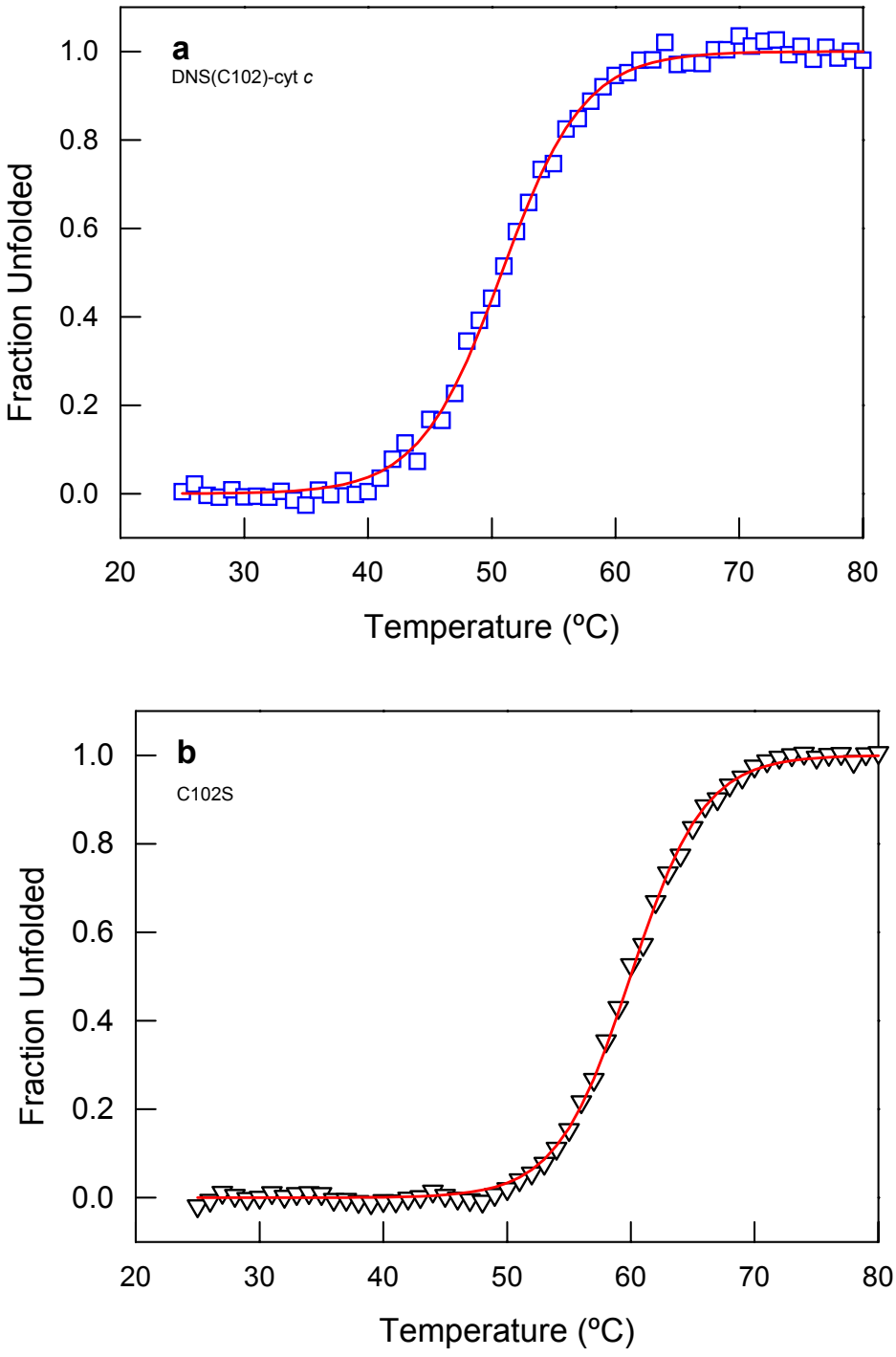

Figure 2.22. CD melting curves for (a) DNS(C102)-cyt *c* and (b) C102S cyt *c*. The transition temperatures are T_m = 51ºC for DNS(C102)-cyt *c* and T_m = 59ºC for C102S cyt *c*.

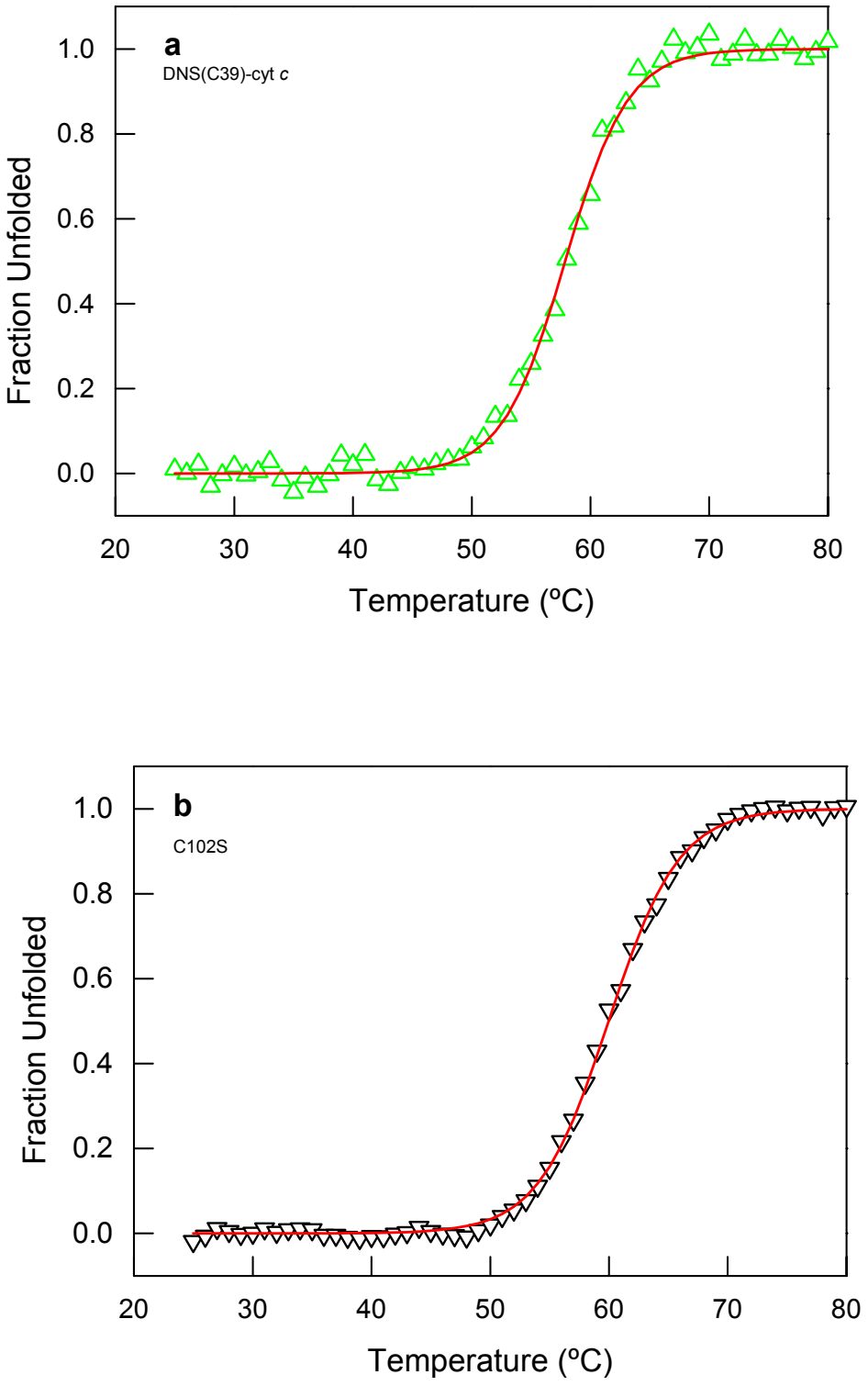

Figure 2.23. CD melting curves for (a) DNS(C39)-cyt *c* and (b) C102S cyt *c*. The transition temperatures are T_m = 58ºC for DNS(C39)-cyt *c* and T_m = 59ºC for C102S cyt *c*.

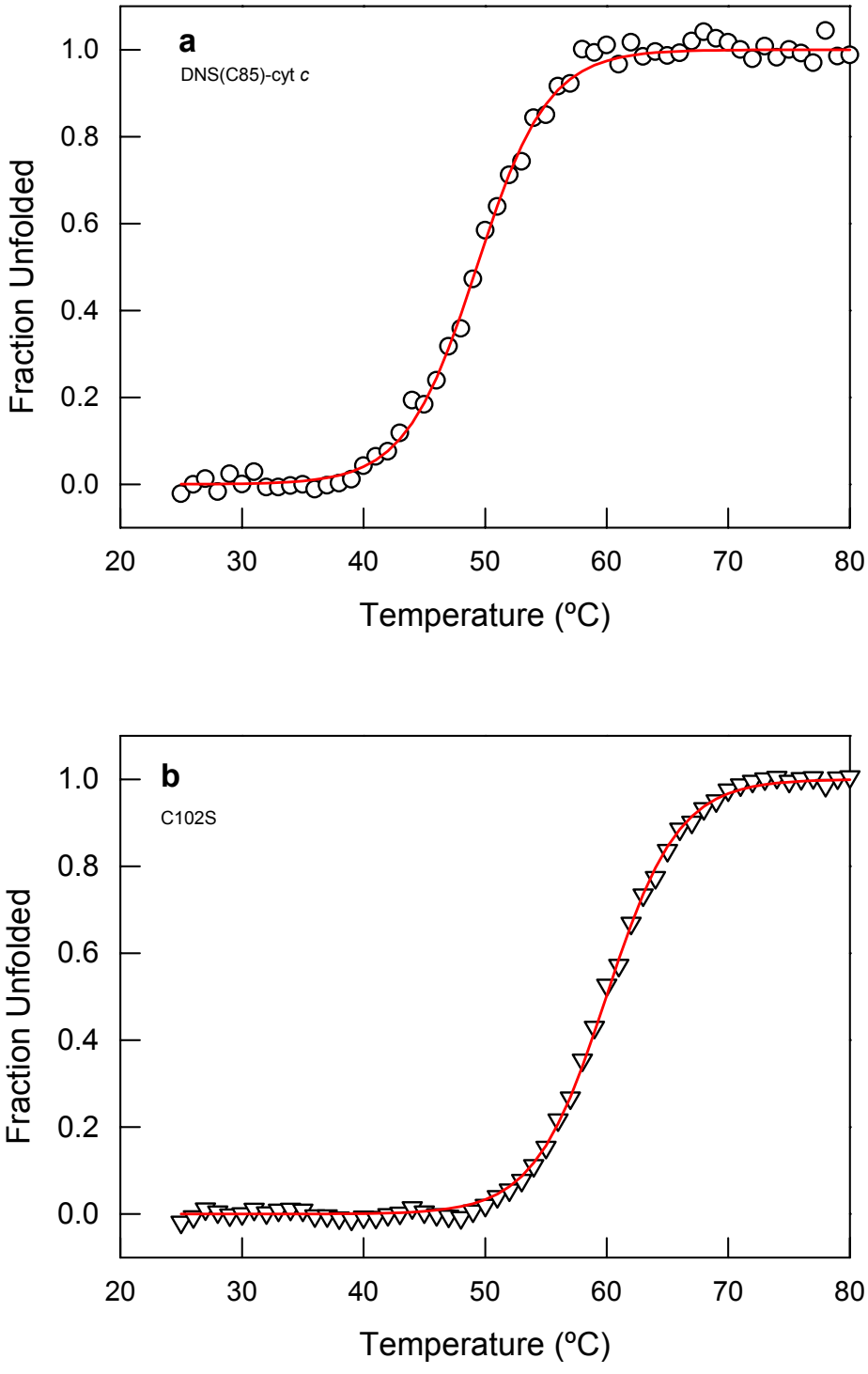

Figure 2.24. CD melting curves for (a) DNS(C85)-cyt *c* and (b) C102S cyt *c*. The transition temperatures are T_m = 49ºC for DNS(C85)-cyt *c* and T_m = 59ºC for C102S cyt *c*.

Equilibrium Unfolding Curves

The UV-VIS and fluorescence spectral changes that accompany guanidinium hydrochloride unfolding of DNS(C102)-cyt *c* are shown in **Figure 2.25.** The blue shift of the Soret band (2 nm, λ_{max} = 408 nm) is accompanied by an increase in the extinction coefficient. The band at 695 nm disappears (not shown), which is interpreted as a loss of axial ligation to the heme iron by thioether sulfur (M80). The nitrogenous base of an amino acid side chain (pH 7: H26, H33, H39) replaces M80 in the guanidinium hydrochloride unfolded protein.[20] Unfolded DNS(C102)-cyt *c* thus remains low-spin. The fluorescence intensity of the DNS group (~500 nm) is strongly quenched in the folded DNS(C102)-cyt *c* due to the energy transfer to the heme group. An increase in the guanidinium hydrochloride concentration leads to a dramatic increase in the fluorescence intensity of the DNS group. Due to a statistical proximity of the DNS fluorophore to the heme even in the unfolded protein, the increase is more moderate in DNS(C39)-cyt *c*, compared to DNS(C102)-cyt *c* and DNS(C85)-cyt *c* .

The unfolding curve for DNS(C102)-cyt *c* is shown in **Figure 2.26**. The midpoint transition for the oxidized form of protein occurs at 0.8 (1) M GuHCl. For the reduced form of protein it is at 3 M GuHCl (Jason Telford, unpublished results). Both, the oxidized and the reduced forms of DNS(C102)-cyt *c* are less stable then those of *S. cerevisiae* iso-1 cytochrome *c* C102S mutant, (y-cyt^{III} $[GuHCl]_{1/2}$ = 1.3(1); y-cyt^{II} $[GuHCl]_{1/2}$ = 3.8(1) at 22.5°C)[21] which is most likely due to some perturbation of the cyt *c* structure near the DNS label. The thermodynamic parameters observed for all DNScyt *c* are summarized in **Table 2.1** (unfolding curves, **Figure 2.26, Figure 2.27, Figure 2.28**). The stability of DNS(C39)-cyt *c* is comparable to that of *S. cerevisiae* iso-1 cytochrome *c* C102S mutant.[21]

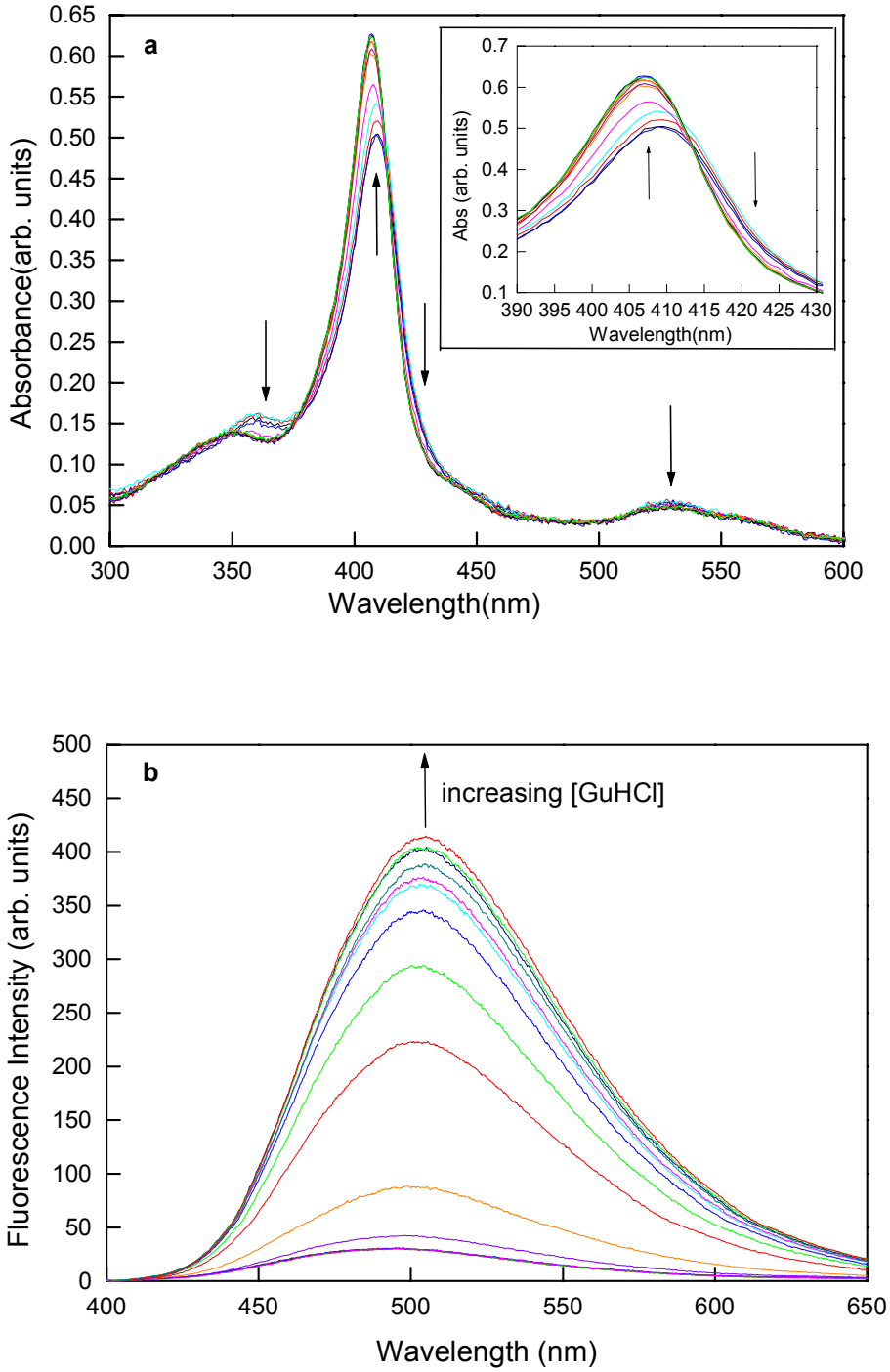

Figure 2.25. (a) Absorption spectral changes during unfolding of DNS(C102)-cyt *c*. Inset is a closeup of the Soret region. (b) Unfolding of DNS(C102)-cyt *c* monitored by DNS fluorescence intensity (λ_{ex} = 355 nm).

Figure 2.26. Equilibrium unfolding data for DNS(C102)-cyt *c* (22.5°C, pH 7). (a) Unfolding curve determined from DNS fluorescence intensity at 500 nm (circles) and absorbance at 400 nm (squares). Lines are the fits to Eq. 2.13. (b) Plot of ΔG_f vs. [GuHCl] (Eq. 2.12).

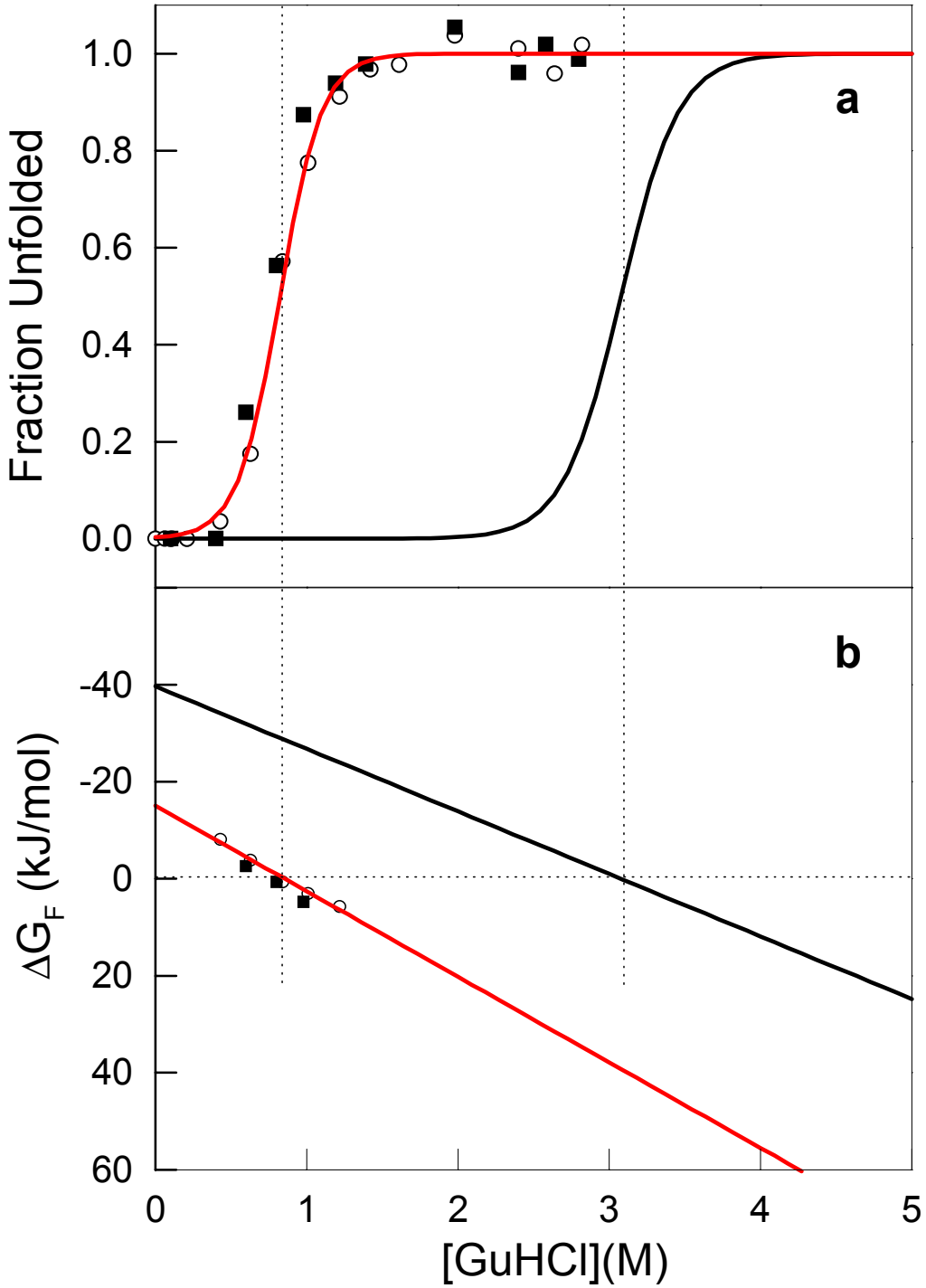
Fraction Unfolded
1.0
0.8
0.6
0.4
0.2
0.0
a
b
-40
-20
0
20
40
60
ΔG_F (kJ/mol)
0
1
2
3
4
5
[GuHCl](M)

Figure 2.27. Equilibrium unfolding data for DNS(C85)-cyt *c* (22.5°C, pH 7). (a) Unfolding curve determined from DNS fluorescence intensity at 500 nm (circles) and absorbance at 400 nm (squares). Lines are the fits to Eq. 2.13. (b) Plot of ΔG_f vs. [GuHCl] (Eq. 2.12).

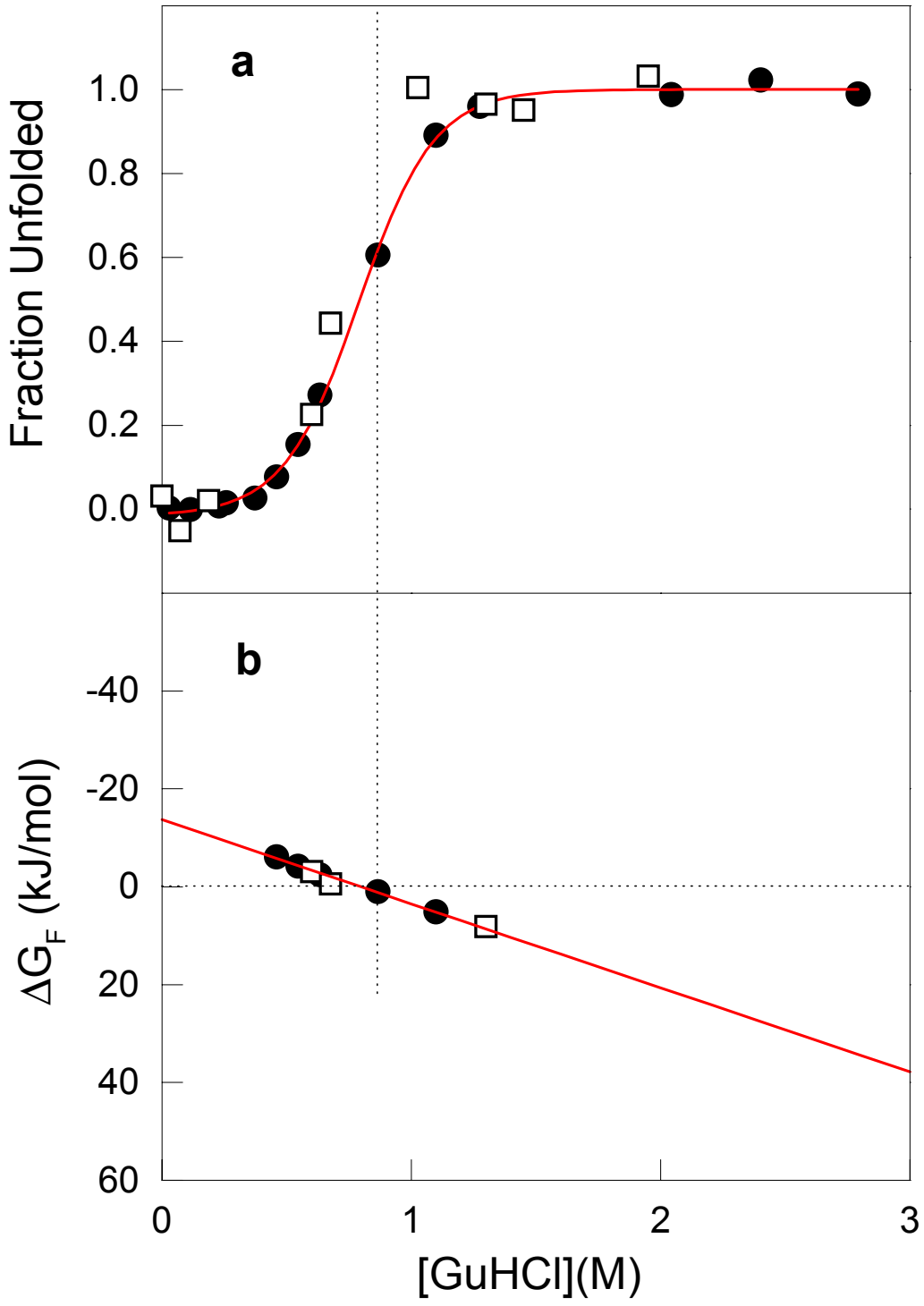
a
b
Fraction Unfolded
1.0
0.8
0.6
0.4
0.2
0.0
-40
-20
0
20
40
60
ΔG_F (kJ/mol)
0
1
2
3
[GuHCl](M)

Figure 2.28. Equilibrium unfolding data for DNS(C39)-cyt *c* (22.5°C, pH 7). (a) Unfolding curve determined from CD at 222 nm (circles) and absorbance at 400 nm (squares). Lines are the fits to Eq. 2.13. (b) Plot of ΔG_f vs. [GuHCl] (Eq. 2.12).

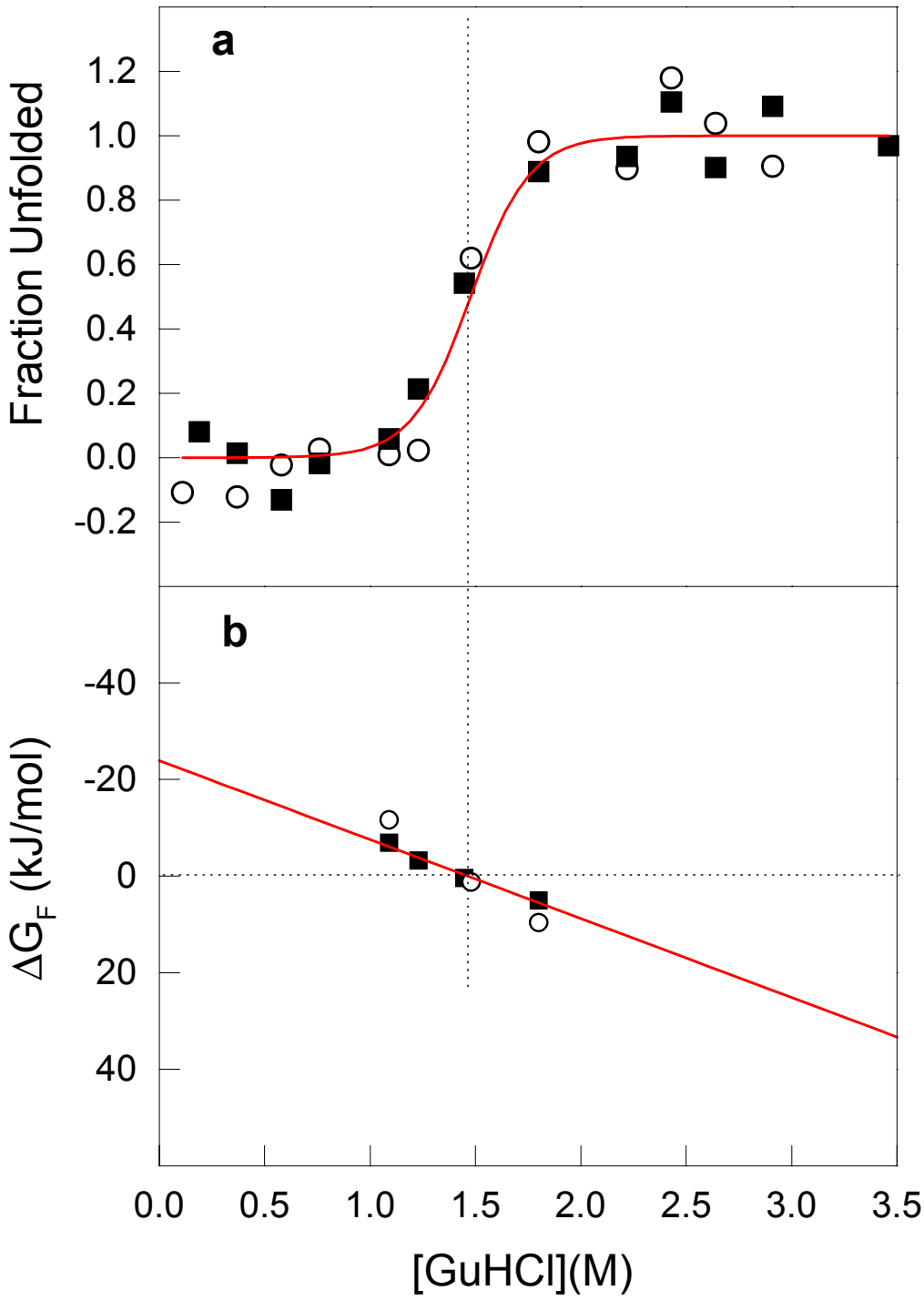
a
b
Fraction Unfolded
1.2
1.0
0.8
0.6
0.4
0.2
0.0
-0.2
-40
-20
0
20
40
ΔG_F (kJ/mol)
0.0
0.5
1.0
1.5
2.0
2.5
3.0
3.5
[GuHCl](M)

Table 2.1 Thermodynamic parameters for DNS(C102)-cyt *c*, DNS(C85)-cyt *c* and DNS(C39)-cyt *c* folding and unfolding.[a]

Protein	T (ºC)	$[GuHCl]_{1/2}$ (M)	$-\Delta G_f^{\circ}$ (kJ mol^{-1})	m_D (kJ mol^{-1} M^{-1})
DNS(C102)-cyt c^{III}	22.5	0.8 (1)	15 (1)	18 (2)
[b]DNS(C102)-cyt c^{II}	22.5	3	39	13
DNS(C85)-cyt c^{III}	22.5	0.8 (1)	14 (2)	17 (10)
DNS(C39)-cyt c^{III}	22.5	1.4 (1)	24 (1)	18 (6)

[a] Numbers in parentheses are estimated uncertainties.
[b]Jason R. Telford, unpublished results.

FET Kinetics

The Förster Distance

The value of $J = 5.5 \times 10^{14}$ $M^{-1}cm^{-1}nm^4$ (Eq. 2.3) was determined from the overlap of the 1,5 NAC-AEDANS fluorescence and cytochrome *c* absorption spectra (**Figure 2.29**). The quantum yield (Φ_D) was 0.3. For the random orientation of donor and acceptor ($\kappa^2 = {}^2/_3$), the critical length (r_0) was 39 Å. The decay of a 1,5 NAC-AEDANS model compound was found to be a single exponential with a decay time of 10.2 ns ($k_0 = 9.81\times10^7$ s^{-1}). The DNS-heme energy-transfer pair was determined to be useful for measuring distances 12 to 60 Å.

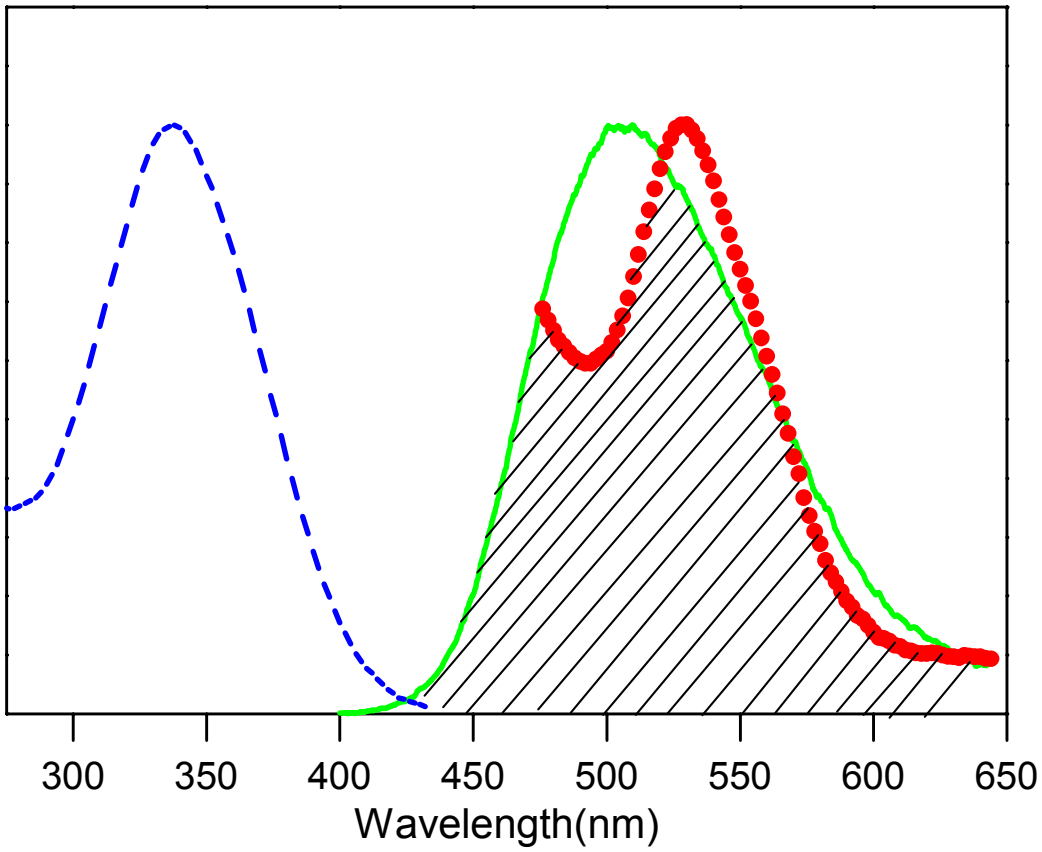

Figure 2.29. Emission (—) of DNS label and absorption spectra of DNS label (---) and heme (circles).

DNS(C102)-cyt *c*

In the folded protein, DNS(C102)-cyt *c* FET kinetics (**Figure 2.30**) transform into a distribution function with a mean ***D-A*** distance of 25 Å and a full-width at half-maximum (FWHM) of about 5 Å (**Figure 2.31**). Addition of GuHCl (<0.5 M) leads to an increase in DNS fluorescence, owing to an increase in the breadth of the distribution centered at 25 Å, along with the appearance of a small population of polypeptide with $\bar{r} > 50$ Å.

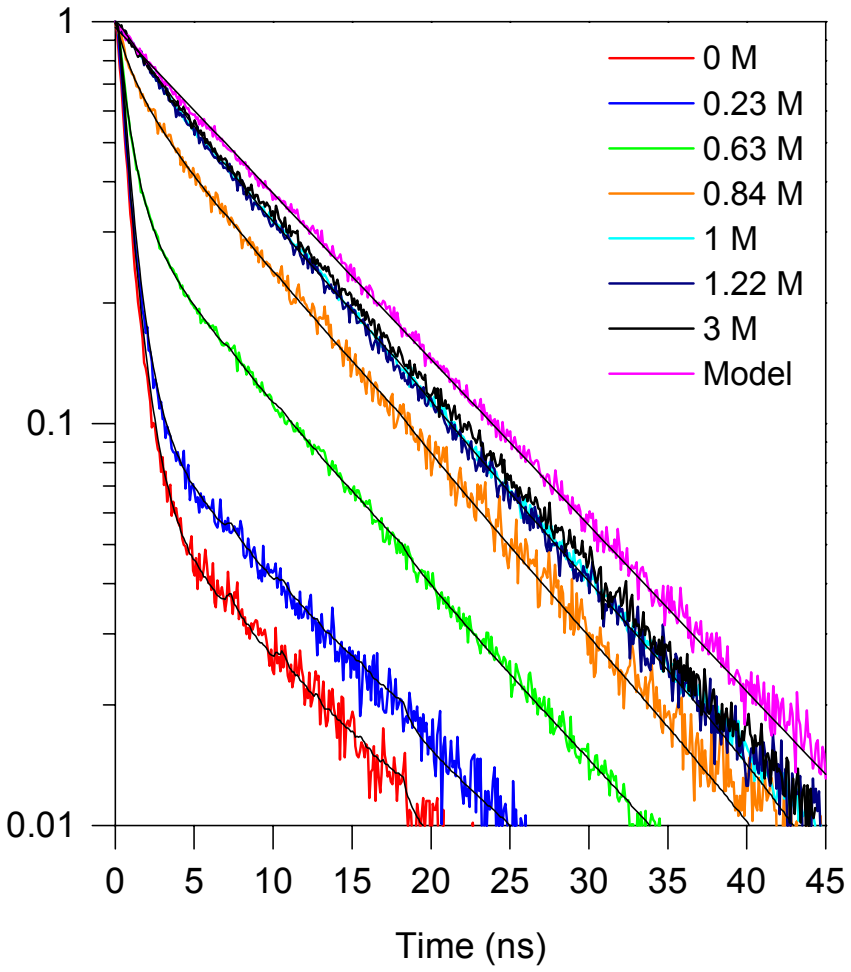

Figure 2.30. Lifetimes observed during equilibrium unfolding of DNS(C102)-cyt *c*. Lines through the data are the results of maximum entropy fits. For the model compound the line is a result of a single exponential fit.

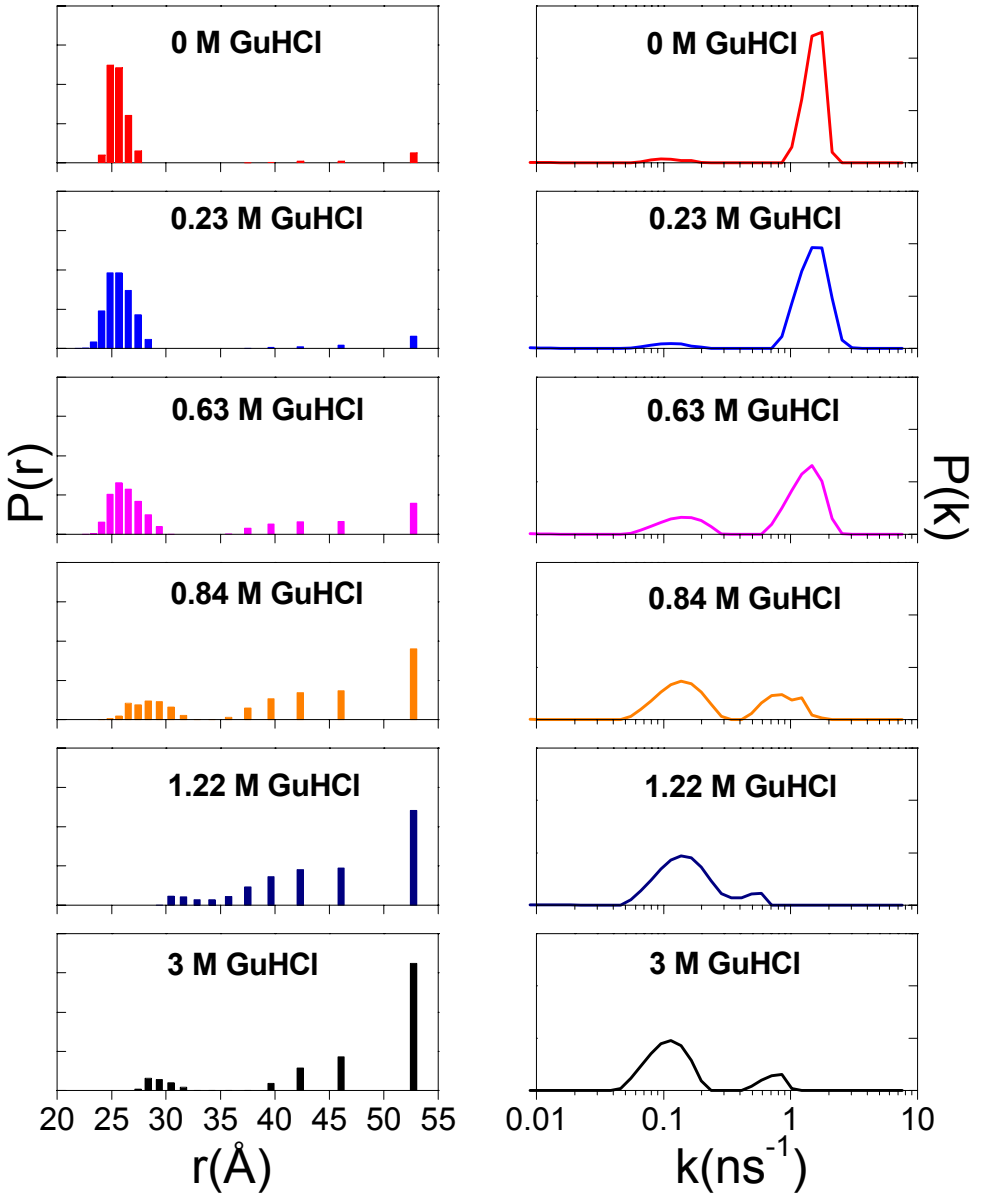

Figure 2.31. GuHCl induced changes in the distribution of luminescence decay rates (*P(k)*, right) and ***D-A*** distances (*P(r)*, left) in DNS(C102)-cyt *c* (pH 7, 22°C). Kinetics data fit using ME algorithm.

The 40-Å critical length limits the ***D-A*** distances that can be measured in unfolded DNS(C102)-cyt *c*, and prevents us from obtaining accurate distributions at large *r* values. Consequently, the single bars at 53 Å in the distributions represent the populations of peptides with $r \geq 53$ Å. As [GuHCl] increases above 0.5 M, the small-*r* distribution loses amplitude as it broadens and moves to a slightly larger mean value ($\bar{r}$ about 29 Å). There is a concomitant increase in the amplitude of the $\bar{r} > 50$ Å population. Finally, at high [GuHCl] (>1.2 M), most of the protein is in an extended conformation ($r > 40$ Å), although a small fraction (about 10%) retains a more compact structure with $\bar{r}$ about 29 Å. Addition of imidazole at high denaturant concentrations has no effect on this compact species. The GuHCl-induced variations in the distribution of ***D-A*** distances are consistent with cooperative unfolding of DNS(C102)-cyt *c*, but the FET kinetics reveal structural features that are not apparent from steady-state spectroscopic measurements.

DNS(C85)-cyt *c*

In the folded protein, DNS(C85)-cyt *c* FET kinetics (**Figure 2.32**) transform into a distribution function with a mean ***D-A*** distance of 20 Å and a full-width at half-maximum (FWHM) of about 5 Å (**Figure 2.33**). A small fraction (about 10%) of protein adopts a slightly more extended configuration with $\bar{r}$ about 30 Å. Upon addition of GuHCl (0.28 M) the 20-Å distribution loses amplitude, the 30-Å population increases and a small population of polypeptides with $\bar{r} > 50$ Å appears. As [GuHCl] increases above the midpoint (0.8 M), the small-*r* distributions collapse to a single broader distribution centered at $\bar{r}$ about 30 Å.

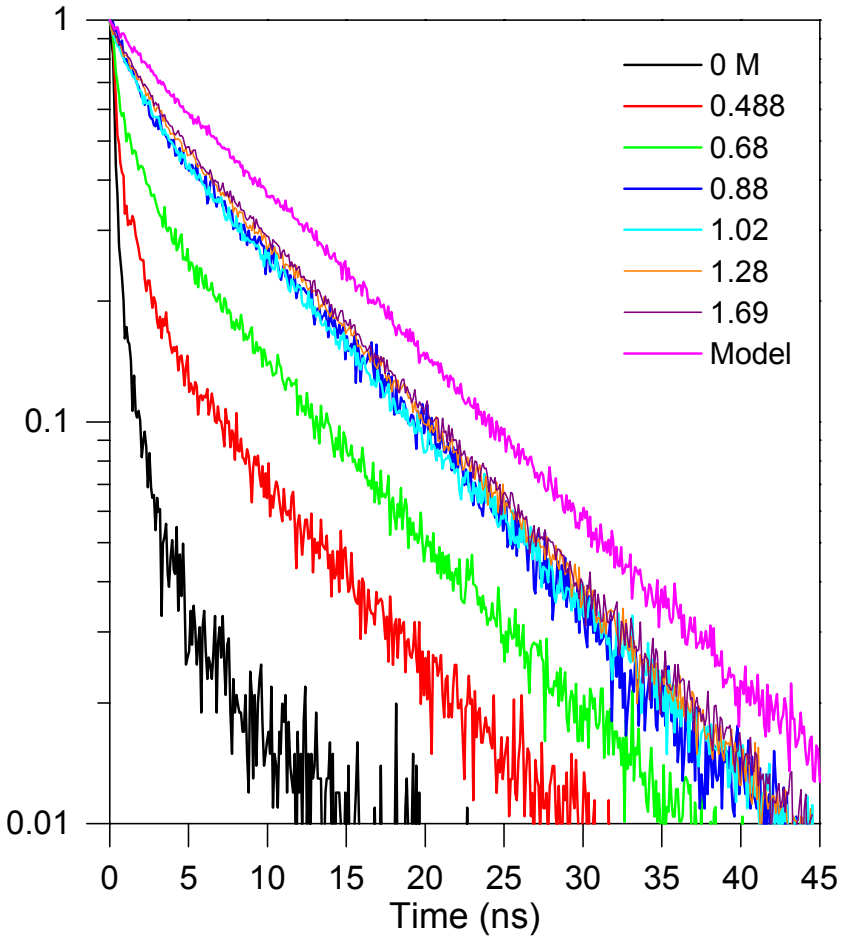

Figure 2.32. DNS fluorescence decay kinetics measured during equilibrium unfolding of DNS(C85)-cyt *c*.

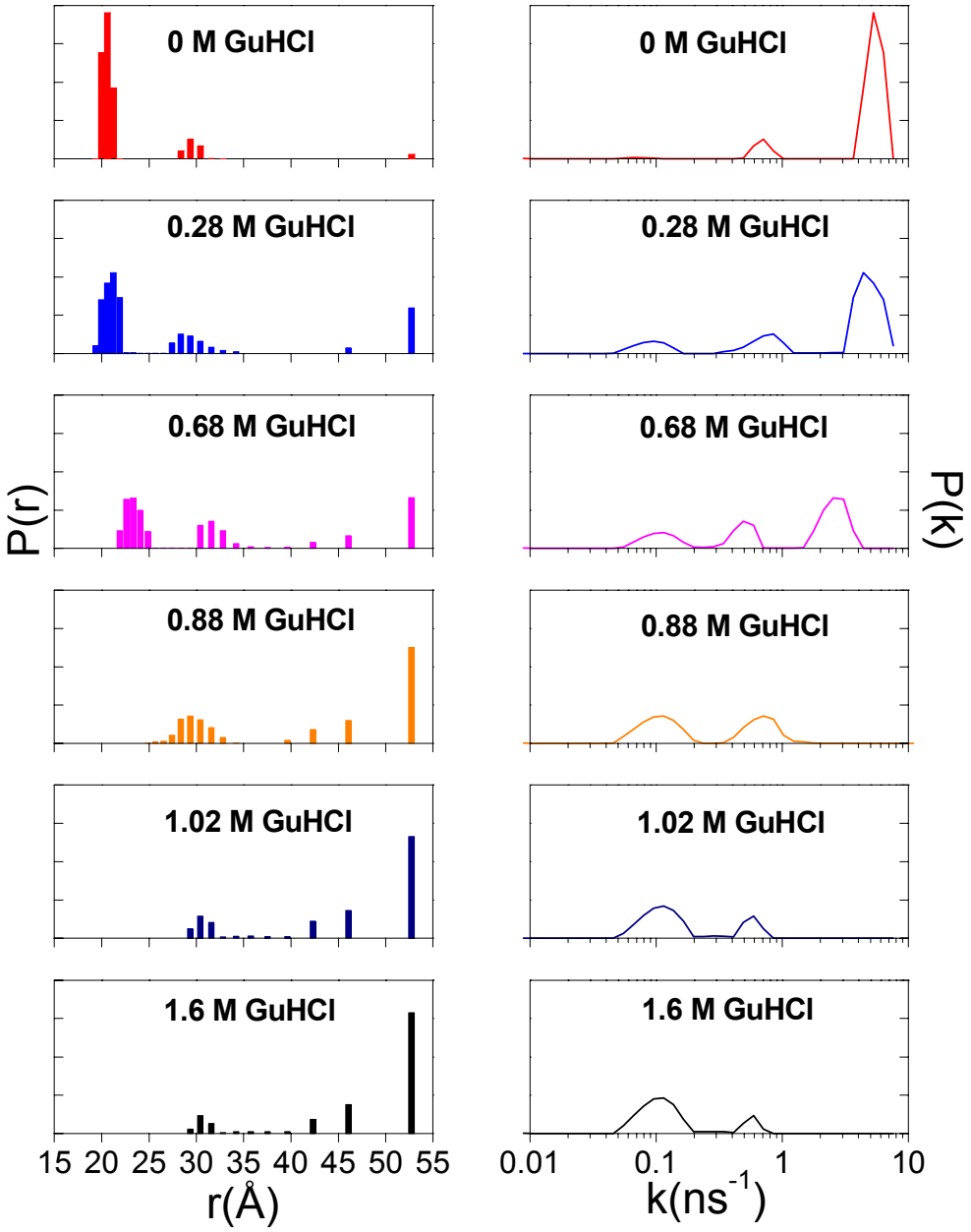

Figure 2.33. GuHCl induced changes in the distribution of luminescence decay rates (*P(k)*, right) and ***D-A*** distances (*P(r)*, left) in DNS(C85)-cyt *c* (pH 7, 22°C). Kinetics data fit using ME algorithm.

As for DNS(C102)-cyt *c*, at high [GuHCl] (>1.2 M), most of the protein is in an extended conformation (r > 40 Å), although a small fraction (about 10%) retains a more compact structure with $\bar{r}$ about 29 Å.

DNS(C39)-cyt *c*

In the DNS(C39)-cyt *c*, the DNS fluorophore is statistically much closer to the heme in the unfolded protein than in either DNS(C102)-cyt *c* or DNS(C85)-cyt *c*. Hence, the overall unfolding detected by FET kinetics is very different from the DNS(C102)-cyt *c* and DNS(C85)-cyt *c*. In the folded protein, DNS(C39)-cyt *c* FET kinetics (**Figure 2.34**) transform into a distribution function with a mean ***D-A*** distance of 23 Å and a full-width at half-maximum (FWHM) of about 5 Å (**Figure 2.35**). Addition of GuHCl (<1.2 M) has no effect on the 23 Å-r distribution and produces no increase in DNS fluorescence. Only as [GuHCl] passes the midpoint (1.4 M), the 23-Å distribution loses amplitude, broadens and moves to a slightly larger mean value ($\bar{r}$about 25 Å); there is a concomitant increase in the amplitude of a 38-Å population. As [GuHCl] increases further, the small-r distribution continues to lose amplitude, broadens, and moves to a larger mean value ($\bar{r}$ about 28 Å). There is a concomitant increase in the amplitude, broadening, and shifting to a slightly larger mean value of the 38-Å population. At very high [GuHCl] (3 M-6 M), about 60% of the protein is in extended conformations ($\bar{r}$ about 40 Å), however a significant fraction (about 40%) retains a more compact structure with $\bar{r}$ about 28 Å. Addition of imidazole at high denaturant concentrations has no effect on this compact species.

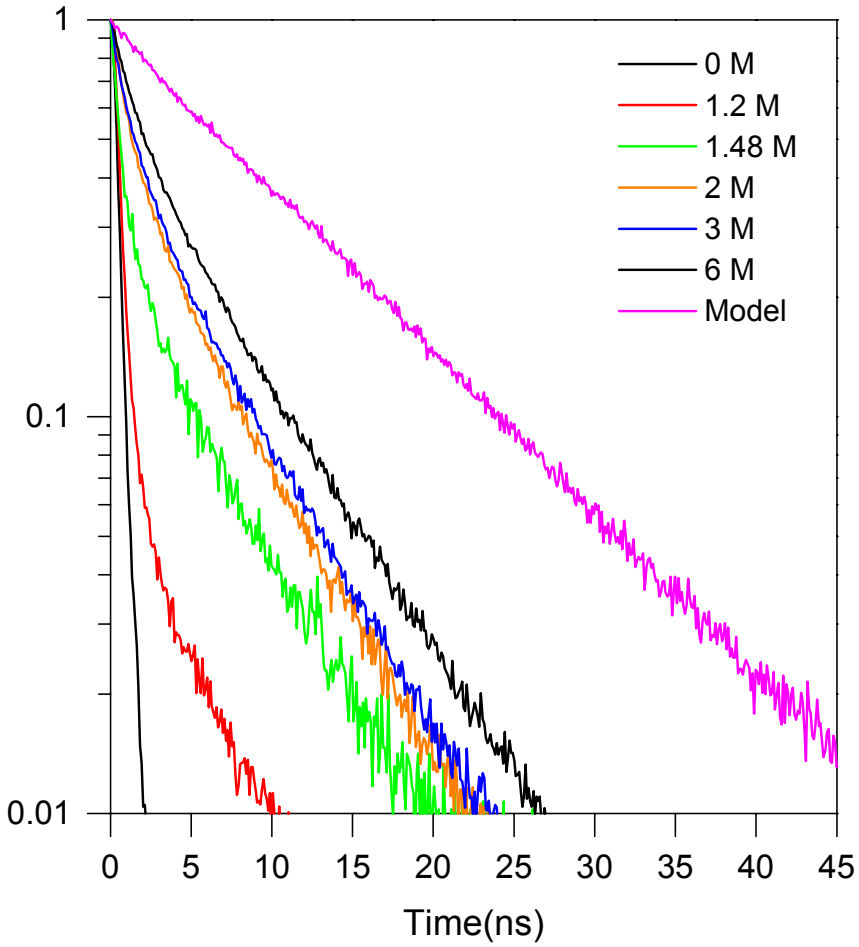

Figure 2.34. DNS fluorescence decay kinetics measured during equilibrium unfolding of DNS(C39)-cyt *c*.

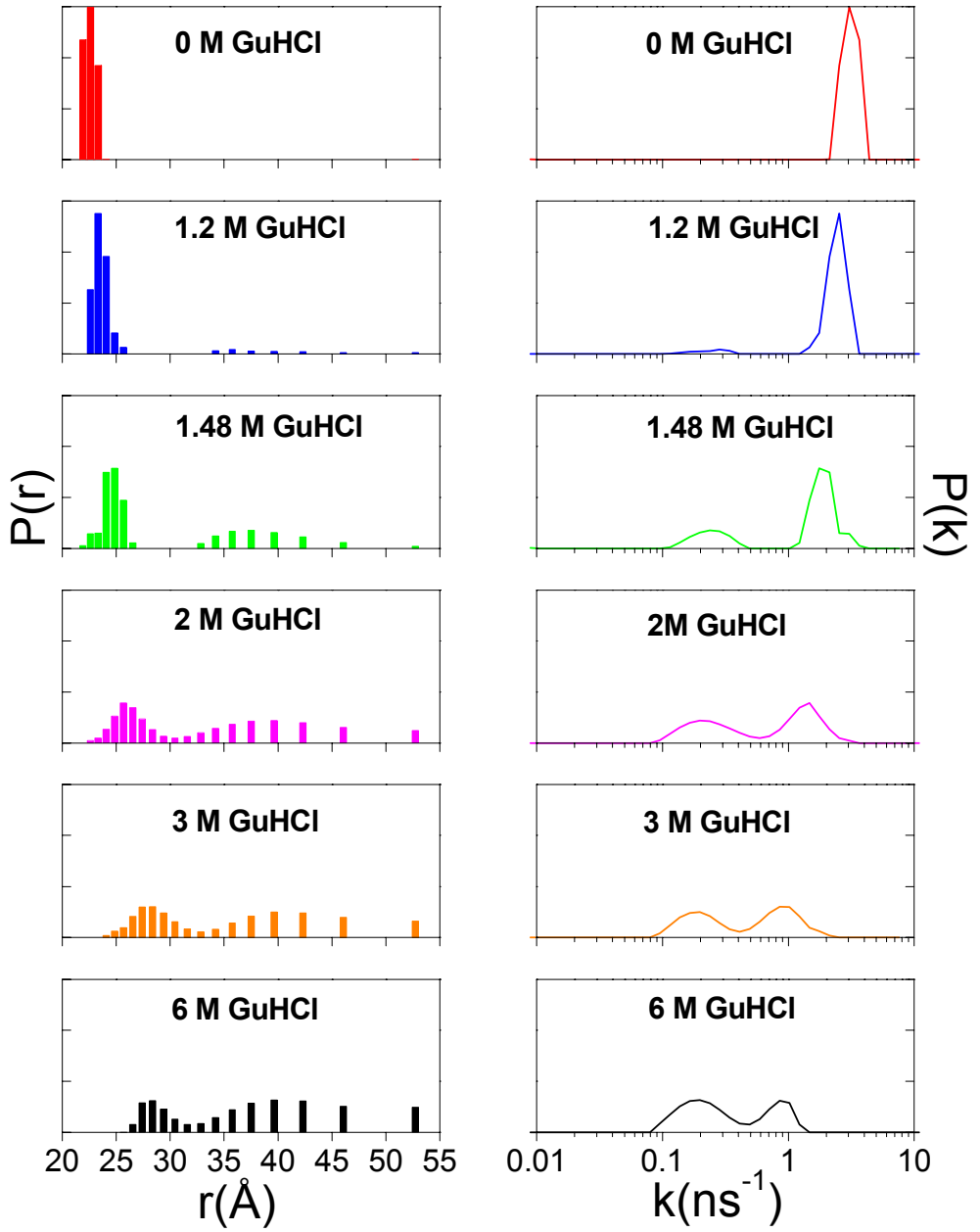

Figure 2.35. GuHCl induced changes in the distributions of luminescence decay rates (*P(k)*, right) and ***D-A*** distances (*P(r)*, left) in DNS(C39)-cyt *c* (pH 7, 22°C). Kinetics data fit using ME algorithm.

The GuHCl-induced variations in the distribution of ***D-A*** distances are consistent with cooperative unfolding of DNS(C102)-cyt *c*, DNS(C85)-cyt *c* and DNS(C39)-cyt *c* but the FET kinetics reveal structural features that are not apparent from steady-state spectroscopic measurements. Consequently, there is a significant fraction of compact molecules (about 40%) in DNS(C39)-cyt *c* at the GuHCl concentrations presumably favoring complete unfolding of the protein (3 to 6 M). This compact fraction is large compared to that in DNS(C102)-cyt *c* (about 10%) and DNS(C85)-cyt *c* (about 10%) under similar conditions.

Segments of the yeast iso-1 cytochrome *c* sequence have been reported to associate with the heme.[13] The region around residue 54 exhibit stronger affinity for the heme, possibly due to a nearby hydrophobic tryptophan residue (position 59). In DNS(C39)-cyt *c* the fluorophore is in a loop containing phenylalanine (position 36) and isoleucine (position 35), and that is also rich in alanine and glycine. Perhaps these nearby hydrophobic and nonpolar residues favor association with the heme thus increasing population of compact molecules. Tryptophan-to-heme FET kinetics[22] reveal increased incidence of compact states in an unfolded ensemble of cytochrome *c*' (about 50%) conceivably due to an increased hydrophobic amino acid content.

Fluorescence Anisotropy Measurements

Upon irradiation of DNS with polarized light, a partially oriented population of *DNS is produced: fluorophores with absorption transition moments parallel to the electric field of the incident light are preferentially excited.[23] Depolarization of the fluorescence occurs as the orientations of *DNS becomes random. For small molecules, the rate of rotational diffusion

is faster than the rate of emission thus giving zero anisotropy. Nonspherical fluorophores attached to biomolecules can exhibit very complex anisotropy decays.[23]

We measured the time-resolved anisotropy decays for DNS(C102)-cyt *c*, DNS(C85)-cyt *c* and DNS(C39)-cyt *c* to determine the rotational freedom of the DNS label in these modified cytochromes. In the folded state, for DNS(C102)-cyt *c*, DNS(C85)-cyt *c*, and DNS(C39)-cyt *c*, the anisotropy decays were described by

$$r(t) = (r_0 - r_\infty)\exp(-t/\tau_c) + r_\infty$$

where the *r(t)* is the total time-dependent anisotropy, τ_c is the rotational correlation time, r_0 is the time-zero anisotropy, r_∞ is the limiting anisotropy. The anisotropy decayed from an initial value of 0.3 to r_∞ = 0.1 with a correlation time of about 1.5 ns (τ_{obs} in the folded protein is about 0.8 ns). The presence of a limiting anisotropy indicates that fluorophore is somewhat hindered and not all rotation angles are available for depolarization.

In the unfolded proteins the anisotropy decays were described by

$$r(t) = \sum_j r_{0j}\exp(-t/\tau_{cj})$$

where the *r(t)* is the total time-dependent anisotropy, r_{0j} are individual anisotropies decaying with the rotational correlation time τ_{cj}. The anisotropy decays were biphasic and decayed from an initial value of 0.2 to zero. The relaxation times were about 230 ps for the fast component and about 1 ns for the slow components. The amplitudes for the two components were comparable.

CONCLUSIONS

Unfolding of different regions of yeast iso-1 cytochrome *c* by GuHCl was monitored by measuring FET kinetics *in situ*. While ensemble-averaged probes (circular dichroism, absorbance, fluorescence intensity, etc.) produced sigmoidal unfolding curves well described by two-state equilibria, FET kinetics revealed structural heterogeneity. We detected various amounts of compact molecules while unfolding different parts of the protein.

The measurements of FET kinetics are effective in detecting structural heterogeneity of the ensemble of protein molecules. Measurements of FET kinetics also revealed heterogeneity in the acid-unfolded DNS(C102)-cyt c and subsequent conversion of the observed complex mixture of conformations into an ensemble of compact ($\bar{r} < 35$ A) polypeptides by high salt concentrations.[24]

The heme is essential to cytochrome *c* folding.[25] In retrospect, the persistence of compact molecules in the denatured ensemble of yeast iso-1 cytochrome *c* and their rapid formation during an early refolding[26] could be explained by this sizeable moiety attracting nearby hydrophobic and non-polar residues.

Supporting Information

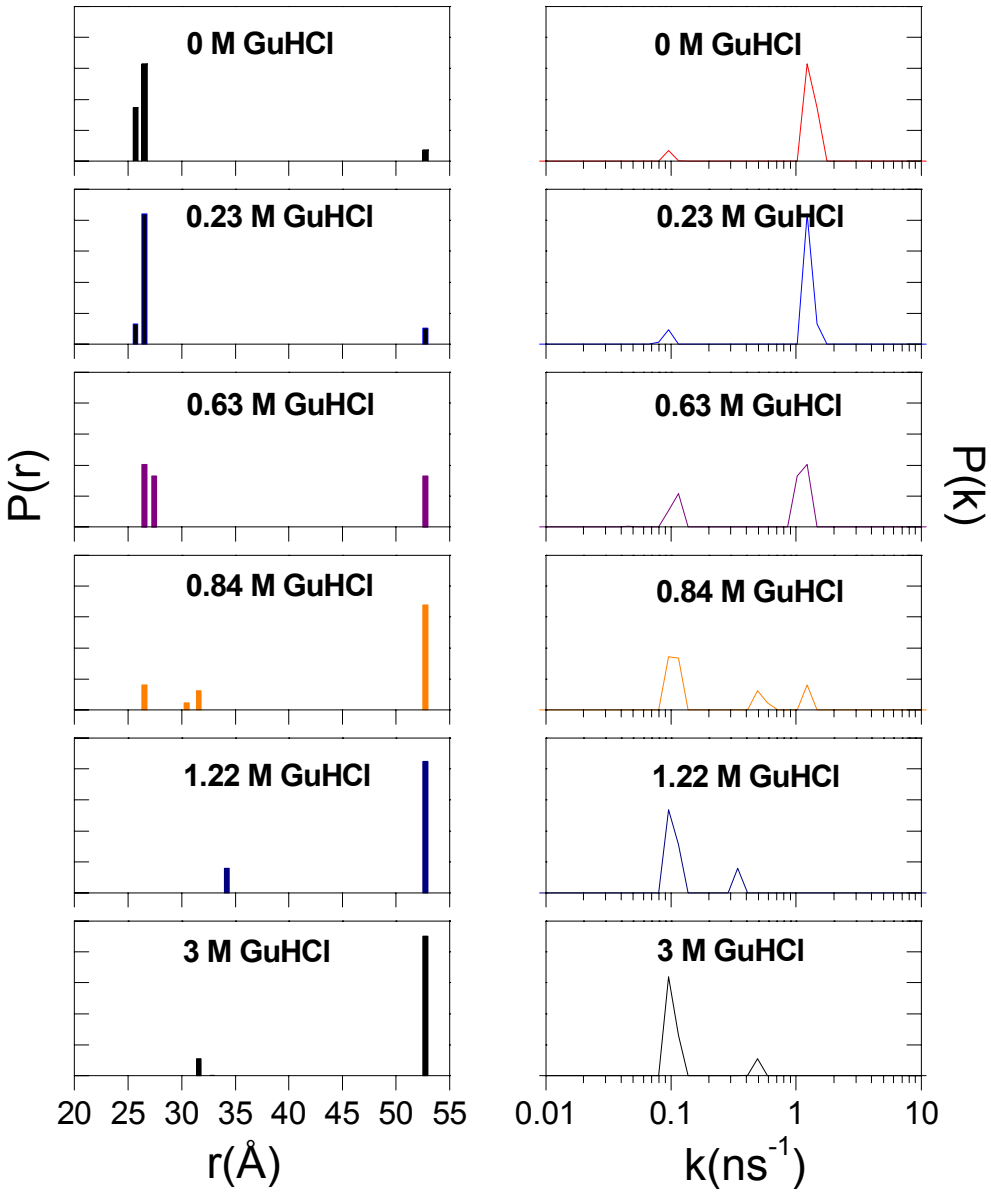

Figure S.2.1. GuHCl induced changes in the distribution of luminescence decay rates (*P(k)*, right) and ***D-A*** distances (*P(r)*, left) in DNS(C102)-cyt *c* (pH 7, 22°C). Kinetics data fit using LSQNONNEG algorithm.

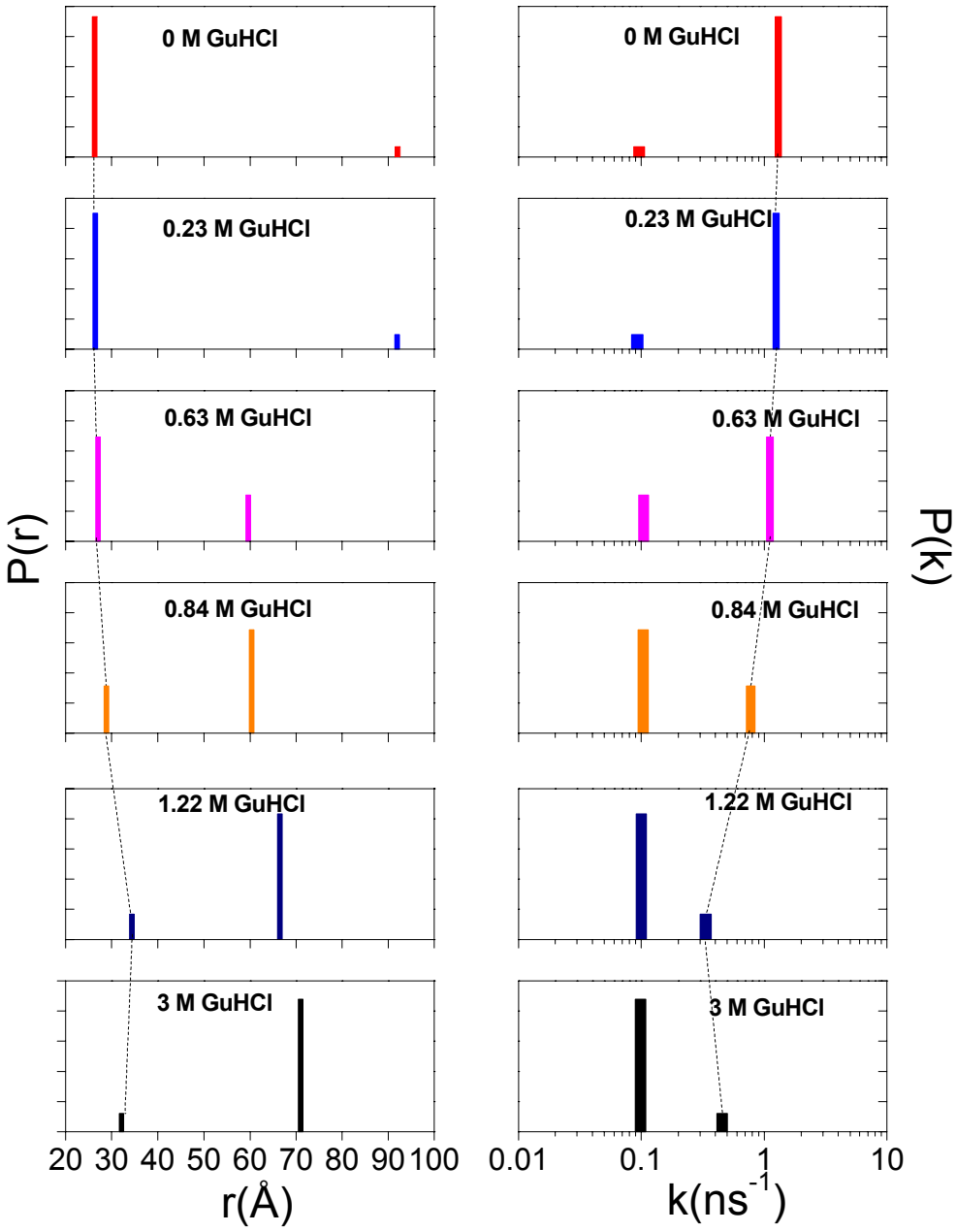

Figure S.2.2. GuHCl induced changes in the distribution of luminescence decay rates (*P(k)*, right) and ***D-A*** distances (*P(r)*, left) in DNS(C102)-cyt *c* (pH 7, 22°C). Kinetics data fit using biexponential algorithm.

REFERENCES AND NOTES

(1) Scott, R. A.; Mauk, A. G. *Cytochrome c—A Multidisciplinary Approach*; University Science Books: Sausalito, 1996.

(2) Navon, A.; Ittah, V.; Landsman, P.; Scheraga, H. A.; Haas, E. *Biochemistry* **2001**, *40*, 105-118.

(3) Moore, G. R.; Pettigrew, G. W. *Cytochromes c: Biological Aspects*; Springer-Verlag: New York, 1987.

(4) Moore, G. R.; Pettigrew, G. W. *Cytochromes c: Evolutionary, Structural, and Physicochemical Aspects*; Springer-Verlag: New York, 1990.

(5) Förster, T. *Ann. Phys. (Leipzig)* **1948**, *2*, 55-75.

(6) Hudson, E. N.; Weber, G. *Biochemistry* **1973**, *12*, 4154-4161.

(7) Inglis, S. C.; Guillemette, J. G.; Johnson, J. A.; Smith, M. *Protein Engineering* **1991**, *4*, 569-574.

(8) McGuirl, M. A.; Lee, J. C.; Lyubovitsky, J.; Thanyakoop, C.; Richards, J. H.; Winkler, J. R.; Gray, H. B. *BBA* **2002**, *1619*, 23-28.

(9) Thöny-Meyer, L.; Künzler, P.; Hennecke, H. *Eur. J. Biochem.* **1996**, *235*, 754-761.

(10) Pollock, W. B. R.; Rosell, F.; Twitchett, M. B.; Dumont, M. E.; Mauk, A. G. *Biochemistry* **1998**, *37*, 6124-6131.

(11) Nozaki, Y. In *Methods in Enzymology*; Hirs, C. H. W., Timasheff, S. N., Ed.; Academic Press: New York, 1972; Vol. 26; pp 43-50.

(12) Godbole, S.; Bowler, B. E. *J. Mol. Biol.* **1997**, *268*, 816-821.

(13) Godbole, S.; Hammack, B.; Bowler, B. E. *J. Mol. Biol.* **2000**, *296*, 217-228.

(14) Bachrach, M. Electron-Transfer in Covalently Coupled Donor-Acceptor Complexes, Caltech, 1996.

(15) O'Connor, D. V.; Phillips, D. *Time-Correlated Single Photon Counting*; Academic Press:, 1984.

(16) *Protein Structure: A Practical Approach*; Creighton, T. E., Ed.; Oxford University Press: New York, 1997, pp 383.

(17) Istratov, A. D.; Vyvenko, O. F. *Rev. Sci. Instrum.* **1999**, *70*, 1233-1257.

(18) Livesey, A. K.; Brochon, J. C. *Biophys. J.* **1987**, *52*, 693-706.

(19) Lawson, C. L.; Hanson, R. J. *Solving Least Squares Problems*; Prentice-Hall: Englewood Cliffs:, 1974.

(19a) The equine cytochrome *c* numbering system is used throughout the text.

(20) Colón, W.; Wakem, L. P.; Sherman, F.; Roder, H. *Biochemistry* **1997**, *36*, 12535-12541.

(21) Mines, G. A.; Pascher, T.; Lee, S. C.; Winkler, J. R.; Gray, H. B. *Chem.& Biol.* **1996**, *3*, 491-497.

(22) Lee, J. C.; Engman, K. C.; Tezcan, F. A.; Gray, H. B.; Winkler, J. R. *Proc. Natl. Acad. Sci. USA* **2002**, *99*, 14778-14782.

(23) Lakowicz *Principles of Fluorescence Spectroscopy*, 2nd ed.; Kluwer Academic/Plenum Publishers:, 1999.

(24) Lyubovitsky, J. G.; Gray, H. B.; Winkler, J. R. *J. Am. Chem. Soc.* **2002**, *124*, 14840-14841.

(25) Fisher, W. R.; Taniuchi, H.; Anfinsen, C. B. *J. Biol. Chem.* **1973**, *248*, 3188-3195.

(26) Lyubovitsky, J. G.; Gray, H. B.; Winkler, J. R. *J. Am. Chem. Soc.* **2002**, *124*, 5481-5485